Sustainable Production and Consumption 70 (2026) 348–363

Contents lists available at ScienceDirect

Sustainable Production and Consumption

journal homepage: www.elsevier.com/locate/spc

Building integrated agriculture as a competitive energy-saving measure: A life-cycle energy assessment☆

Joan Muñoz-Liesa [a,b,c,*], Michael Martin [b,d], Anna Petit-Boix [e], Mélanie Douziech [c], Thomas Nemecek [c], Xavier Gabarrell [e,f], Eva Cuerva [g], Santiago Gassó-Domingo [g], Alejandro Josa [a]

[a] Department of Civil and Environmental Engineering (DECA), School of Civil Engineering (Escola de Camins), Universitat Politècnica de Catalunya (UPC), Jordi Girona 1-3, Barcelona, Spain
[b] Department of Sustainable Development, Sustainability Science and Engineering, School of Architecture and the Built Environment, Royal Institute of Technology (KTH), Sweden
[c] Agroscope, Life Cycle Assessment research group, CH-8046, Zurich, Switzerland
[d] IVL Swedish Environmental Research Institute, Sustainable Society, Stockholm, Sweden
[e] Sostenipra Research Group (2021 SGR000734), Institut de Ciència i Tecnologia Ambientals, Z Building, Universitat Autònoma de Barcelona (UAB), Campus UAB, 08193, Bellaterra, Barcelona, Spain
[f] Department of Chemical, Biological and Environmental Engineering, Universitat Autònoma de Barcelona, Campus UAB, 08193, Bellaterra, Barcelona, Spain
[g] Department of Project and Construction Engineering (EPC), Group of Construction Research and Innovation (GRIC), Universitat Politècnica de Catalunya (UPC), Edifici H, Av. Diagonal, 647, Barcelona, Spain

ARTICLE INFO

Editor: Kuishuang Feng

Keywords:
Building integrated agriculture
Urban agriculture
Life cycle energy assessment
Circular economy
Controlled environment agriculture

ABSTRACT

Building-integrated agriculture (BIA) has emerged as a strategy to decarbonize cities by reusing energy flows between buildings and controlled environment agriculture (CEA). A wide variety of configurations —including rooftop, façade greenhouses and vertical farms— have shown to reduce heating demand by 3–24% through passive energy integration and achieve 10–34% savings when coupled with active ventilation systems. However, most assessments remain theoretical, and little is known about the life-cycle performance of real-world demonstrators. This study applies a life-cycle energy assessment (LCEA) to an integrated rooftop greenhouse (iRTG) in Barcelona to evaluate whether energy circularity reduces life-cycle energy impacts through a set of energy indicators. Results confirm trends observed in the literature: passively ventilated iRTGs provide life-cycle energy gains but come with high embodied energy costs from iRTG's building materials (accounting for 86% of LCEA). Conversely, active configurations reduce building annual energy demand by up to 12% despite higher material and operational inputs. In turn, active iRTGs reach an energy payback time of 2.2 years and an energy return on investment of 22.8, compared to 3.5 years and 14.2 in passive systems. Such values are comparable with those reported for other energy-saving strategies such as building retrofits or photovoltaic panels, highlighting BIA's competitiveness. By combining evidence from prior studies with empirical data from a world demonstrator, this work confirms that energy circularity in BIA can lower life-cycle energy impacts when appropriately designed and integrated. BIA thus represents not only food-producing infrastructures for cities but also viable energy-saving measures that contribute to the decarbonization of the urban building stock.

☆ This article is part of a Special issue entitled: 'Sustainable Urban Transitions' published in Sustainable Production and Consumption.

* Corresponding author at: Department of Civil and Environmental Engineering (DECA), School of Civil Engineering (Escola de Camins), Universitat Politècnica de Catalunya (UPC), Jordi Girona 1-3, Barcelona, Spain.
E-mail address: jmunozliesa@gmail.com (J. Muñoz-Liesa).

https://doi.org/10.1016/j.spc.2026.10.020
Received 25 June 2026; Received in revised form 26 September 2026; Accepted 23 October 2026
Available online 27 October 2026
2352-5509/© 2026 The Authors. Published by Elsevier Ltd on behalf of Institution of Chemical Engineers. This is an open access article under the CC BY license (http://creativecommons.org/licenses/by/4.0/).

1. Introduction

1.1. Energy consumption in buildings and greenhouses

Buildings are among the largest energy consumers worldwide, contributing to one-third of the global greenhouse gas emissions (UNEP, 2007). In Europe, 75% of the buildings are energy inefficient due to their aging stock (European Union, 2018) and thus require urgent upgrades to comply with energy performance standards. Throughout a building's life cycle, heating and cooling are the most energy-intensive processes (Chau et al., 2015; Wallgren and Höjer, 2009), with varying contributions depending on the building's design. In conventional buildings, it can reach up to 90% of energy impacts, where 10–20% are embodied in construction materials (Ramesh et al., 2010). For nearly-zero-emission buildings, total energy use is much lower, and materials represent up to 75–100% of the energy impacts (Chastas et al., 2016). Upgrading the building stock therefore requires a thorough understanding of both embodied and operational energy needs. One innovative approach is building-integrated agriculture (BIA), where greenhouses and other agricultural practices are integrated into buildings, thereby reducing energy demand.

Greenhouses are buildings with transparent envelopes designed to generate ideal environmental conditions that favor plant growth. In response to the growing population and food supply needs, greenhouses have seen a steady growth from 2009 to 2020, doubling their footprint area to reach 2100 km^2 (Eurostat, 2020). However, like other building types, greenhouses face energy and environmental challenges due to their heating and cooling requirements (Torrellas et al., 2012a; JRC, 2015; Stanghellini et al., 2016) and, thus, need a plan to decarbonize (Montero et al., 2012). Improving greenhouse energy efficiency through better insulation can improve operational performance but shifts impacts to the construction phase (Specht et al., 2013). In fact, in unheated greenhouses, greenhouse infrastructures are one of the primary sources of embodied environmental impacts (Torrellas et al., 2012b; Muñoz et al., 2008; Martínez-Blanco et al., 2009), underscoring the importance of holistic design strategies to balance operational and embodied energy demands and environmental impacts.

Building-integrated agriculture, such as urban vertical farms or rooftop greenhouses integrated into buildings, creates opportunities to connect civic life with agriculture (Gould and Caplow, 2012; Proksch, 2017) while allowing for energy savings (Specht et al., 2013). In addition, the environmental conditions promoting plant growth in CEA systems make them ideal systems for reusing of building waste heat and CO_2 flows to produce food year-round (Sturm et al., 2014; Muñoz-Liesa et al., 2021a). This urban symbiosis supports circular economy goals (Petit-Boix and Leipold, 2018) and holds potential to reduce the environmental impacts of both the building and the food produced. This is the case of rooftop greenhouses (RTGs), which, thanks to their bioclimatic function, have the potential to act as solar captors, exploiting the synergies between greenhouses and building waste energy flows. While the bioclimatic effect of passively heated greenhouses favors low-grade heat potentially reusable by buildings, actively heated CEA environments properly integrated with the buildings' heating, ventilation and air conditioning (HVAC) controls can also yield improved energy performances compared to stand-alone buildings and CEA facilities (Jans-Singh et al., 2021).

While reducing primary energy demand is paramount in any building, studies assessing energy circularity (i.e., the directed reuse of thermal energy flows including waste heat and solar gains) between CEA and buildings through BIA systems are scarce (Drottberger et al., 2023). A key barrier to realizing these synergies is the need for stronger stakeholder coordination (Cerón-Palma et al., 2012), since energy circular solutions often require tailored, integrated management of heat flows. Moreover, circular solutions tend to offer sub-optimal conditions for CEA systems (yielding a decrease of crop yields), since they mainly benefit building systems (Martin et al., 2022; Muñoz-Liesa et al., 2020a). Thus, a system-level approach that includes both energy and environmental perspectives is needed to quantify the overall benefits of circular-integrated CEA systems. By doing so, all potential trade-offs between energy synergies and crop productivity in BIA could be considered.

1.2. Research gaps and objectives

Previous research demonstrated that energy circularity in BIA does not necessarily improve the operational energy costs of the integrated buildings. Instead, the design of BIA systems should incorporate appropriate technologies and account for local climatic conditions to maximize energy co-benefits while preventing unforeseen tradeoffs (Hugo et al., 2021). Integrating CEA systems into unused urban spaces is, therefore, a possible way of retrofitting existing buildings and reducing overall energy needs; however, to what extent BIA energy circularity reduces the energy-related impacts of the built environment is still unclear (Haupt and Hellweg, 2019). Moreover, whether the construction-phase burdens of BIA, such as the incorporation of sophisticated active energy controls, can offset the operational benefits over the BIA lifespan remains to be explored (IPCC, 2019). Answering these questions requires real-world data and quantitative environmental metrics, rather than assuming that circularity is inherently beneficial (Haupt and Hellweg, 2019). This would provide indicators to prioritize different energy recovery strategies for improved decision-making, from simple greenhouse structures physically connected with buildings providing passive energy benefits to more sophisticated greenhouse infrastructures with integrated climate controls and the subsequent material inputs needed for active energy systems such as ducts, fans or heat exchangers (Benis et al., 2015).

The objective of this study is threefold: (i) to perform a life cycle energy assessment (LCEA) of BIA; (ii) to balance the lifetime energy-related benefits and costs of implementing CEA systems in buildings using active and passive ventilation strategies, and (iii) to investigate whether the energy circularity of BIA results in improved life cycle energy performance, comparing both active and passive energy systems as well as other building saving and retrofit measures using a set of energy indicators. The novelty of this work lies in three aspects that have not been jointly addressed in prior research: (1) the use of empirical operational data from a real-world BIA demonstrator rather than theoretical simulations alone (which most assessments rely on) as input to an LCEA; (2) the integration of both building and greenhouse life-cycle perspectives within a single system boundary; and (3) the benchmarking of BIA energy performance against established energy-saving retrofit technologies using comparable metrics (energy payback time, EPT; and energy return on investment, EROI). In doing so, this study provides life-cycle evidence that energy circularity in BIA can deliver net life-cycle energy benefits when appropriately designed, moving beyond the current theoretical consensus.

To exemplify the energy metabolism of BIA, the ICTA-ICP office building integrated with four iRTGs is used as a world demonstrator of BIA synergies. This analysis built upon previous assessments that individually addressed the material and energy flows of this building (Muñoz-Liesa et al., 2021a; Muñoz-Liesa et al., 2020a; Muñoz-Liesa et al., 2021b). As a result, it covers life-time energy and material flows for both building and greenhouse perspectives, analyzing (i) iRTGs as a building retrofit solution that operates mainly as solariums, taking advantage of the solar collection capacity of integrated greenhouses to fulfill building heating demands; and (ii) iRTGs as a building sink that can benefit from building waste heat, diversifying energy resources of greenhouses. To this end, we aim to offer a comprehensive understanding of the energy-related impacts of BIA, providing guidelines for future BIA designs to support the decarbonization of the built environment.

2. Current knowledge in BIA energy circularity: a review

Few studies have explicitly quantified the energy benefits of BIA closely integrated into cities. Beyond the urban boundaries, industrial-scale applications of low-grade heat recycled in CEA facilities, such as greenhouses, have previously been assessed and applied (Thomas et al., 2017; SUEZ, 2017) by exploiting the concepts of industrial and urban circularity (Rezaei et al., 2024; Burg et al., 2021). To track studies on the urban settings that explicitly quantify such BIA circular energy benefits, a non-exhaustive review was conducted by tracing peer-reviewed

Table 1
Literature review of case studies, energy modeling approaches and energy savings in BIA thanks to the integration of energy circularity strategies, presented in order of publication. VF stands for vertical farm.

Authors	BIA type & location	Modeling approach	Energy flows	Summary of energy savings due to BIA circularity
Delor, 2011	RTG, Greenwich, London, UK	Preliminary theoretical model (manual calculations)	Unidirectional (RTG > building)	13% energy savings to the host building with active and passive energy means thanks to the RTG when a good roof insulation exists (U = 0.4 W/m^{2}K); up to 41% savings with poor roof insulation (e.g. single glass, U = 8 W/m^{2}K)
Cerón-Palma et al., 2012	RTG, Cabrils, Barcelona, Spain	Theoretical model (EnergyPlus)	Bidirectional	3–5% passive energy savings to the host building in winter; up to 79% building energy savings with active and passive energy means of daily benefits in winter.
Sdringola et al., 2014	Façade-integrated bioclimatic greenhouses, Perugia, Umbria, Italy	COMSOL Multiphysics™ (a CFD - FEM software)	Unidirectional (greenhouse > building)	20% passive energy savings to the host building during heating season (October–April). Shading devices to lower temperatures up to 27% during summer.
Nadal et al., 2017a, 2017b	RTG and the ICTA-UAB office building, Barcelona area, Spain	The theoretical model (EnergyPlus) is based on experimental facilities.	Unidirectional (building > RTG)	40% of energy savings compared to soil-based greenhouses, equivalent to 342 kWh/m^2·y of energy, was recycled in the RTG from the host building, performing 34% thermally better than a soil-based greenhouse.
Syed and Hachem, 2019	Façade-integrated greenhouse in a food retail building in Calgary, Canada.	Theoretical model (EnergyPlus)	Unidirectional (building > building + greenhouse)	21% active heating energy savings of the greenhouse-retail complex. This results from the surplus waste heat from the refrigeration compressor rack used to cool freezers from the food retail actively conveyed in the HVAC systems otherwise rejected to the outside.
Muñoz-Liesa et al., 2020a, 2020b	RTG and the ICTA-UAB office building, Barcelona area, Spain	The theoretical model (EnergyPlus) is based on experimental facilities.	Bidirectional	4% passive annual energy savings to the host building, representing 120 kWh/m^2 net savings on energy demand (118 kWh/m^2 in heating, 8 kWh/m^2 in cooling).
Gholami et al., 2020	RTG, Bologna, Italy	WUFI software (Wärme Und Feuchte Instationär for 2D hygrothermal simulation)	Unidirectional (RTG > building)	15% passive energy savings for the host building, also thanks to the soil insulation of the greenhouse.
Jans-Singh et al., 2021	RTG and school building, London, UK	Theoretical model (Matlab and EnergyPlus)	Bidirectional (with actively heated RTG)	1% passive energy savings to the host building, 9–10% considering the RTG occupies the entire building roof. 3% increase of total energy demand with actively-heated RTG
Hugo et al., 2021	RTG, Tshwane, South Africa	Simulation model (ENVImet, IESve), based on experimental RTGs (plastic structures, not integrated)	Unidirectional (RTG > building)	0.73 °C decrease in mean temperature for passive RTG in a highly insulated building roof (U = 0.266 W/m^{2}K), leading to a 3.5% increase of building energy consumption (11% under a future climate change scenario), 3.1% increase for poorly insulated building roofs (U = 0.841 W/m^{2}K).
Muñoz-Liesa et al., 2021a	RTG and the ICTA-UAB office building, Barcelona area, Spain	The theoretical model (EnergyPlus) is based on experimental facilities.	Bidirectional	8–19% active energy savings to the host building, representing 205 kWh/m^2 y average savings on energy demand. 198 kWh/m^{2}y of average thermal heat could be harvested from the building to the RTG.
Ledesma et al., 2021	RTG and school building in Quito, Ecuador	Theoretical model accounting plants evapotranspiration (Matlab and EnergyPlus)	Unidirectional (RTG > building)	19% of passive energy savings to the host building with 1–2 stories and poorly insulated roof (U = 1.00—1.34 W/m^{2}K) representing 42–48% of heating energy savings. 13–16% of building energy savings with active ventilation systems due to the 7% additional electricity needs.
Yeo et al., 2022	RTG integrated into an office building in Seoul, South Korea	The theoretical model includes computational fluid dynamics and TRNSYS software	Unidirectional (building > RTG)	5.2% annual reduction in energy load of the single-span RTG. By altering the greenhouse temperature, 11.8% of energy savings were achieved from November to March.
Martin et al., 2022	VF integrated underneath a building in Hammarby Sjöstad, Stockholm, Sweden	Manual theoretical energy calculations (Microsoft Excel) based on primary energy data	Unidirectional (VF > neighborhood)	16% of active energy savings to VFs corresponding to 106 MWh of waste heat from LEDs systems was calculated to displace district heating needs, otherwise rejected to the outside through an air cooler.
Blom et al., 2023	VF and different host buildings in the Netherlands	Manual theoretical energy calculations (Microsoft Excel) based on secondary energy data	Bidirectional	12–34% of active energy savings to VFs and their host buildings, depending on the type of integration. Host buildings with continuous energy demand (e.g. swimming pools) could reduce energy demands by up to 51%.
Blom et al., 2024	VF and different host buildings in Amsterdam, the Netherlands	Manual theoretical energy calculations (Microsoft Excel) based on primary energy data	Unidirectional (VF > neighborhood)	15% of energy savings to VFs provided to the district heating network in a decentralized heat pump configuration, like data centers' advantages.
Choi et al., 2024	RTG build on top of a shipping metal container in Daejeon, South Korea	Theoretical model for Building Energy Simulation (BES), TRNSYS software.	Bidirectional	0.7–4.0% passive energy savings for the RTG, 6.3% savings with active ventilation systems. 18.4–24.7% passive energy savings for the building (container). 11.4% of overall energy savings for the RTG-building system, compared to isolated greenhouses and buildings.

articles containing keywords such as “building integrated agriculture”, “urban agriculture”, “rooftop greenhouses” or “circularity”. Other relevant sources were found following a snowball approach, tracing citations from the first set of articles found. As a result, while first assessments started in 2011, a growing number of studies have been published between 2020 and 2024, summing up a total of 16 assessments (Table 1). Most of the studies (12 out of 16) focused on integrated greenhouses in building facades (2) and rooftops (10). This is due to greenhouses' bioclimatic function, which traps solar energy that can be passively or actively conveyed to buildings when physically integrated, thus enhancing BIA's energy circularity. However, the quantifiable benefits vary based on local characteristics, including weather conditions, building and greenhouse ventilation strategies, relative humidity, temperature setpoints, and the number of building levels attached to an iRTG.

Such local characteristics show that the passively energy-related benefits of iRTGs can save between 3 and 15% of the host building's heating demand with standard roof insulations (Jans-Singh et al., 2021; Muñoz-Liesa et al., 2020a; Doeschate, 2015; Cerón-Palma, 2012; Gholami et al., 2020), and up to 20% during the heating season (Sdringola et al., 2014). Benis et al. (2015) highlighted the influence of the roof insulation capacity of the building when calculating energy co-benefits of iRTGs, since lower thermal insulation (i.e., greater U-values) enhances heat flux exchanges. As a result, the energy benefits of passive heating tend to increase by up to 18–24% (Ledesma et al., 2021; Choi et al., 2024) only in cases where iRTGs have poorly insulated roofs ($>$ 0.8 W/m^{2}K) (Ledesma et al., 2021; Delor, 2011). This is important considering the uninsulated building stock in Europe. In Spain, for instance, 76% of building rooftops have a U-value as high as 1.0–1.8 W/m^{2}K, whereas 24% have an improved value between 0.4 and 0.5 W/m^{2}K (for buildings dating from 2000 onwards) (European-Commission, 2016). Similarly, using active systems in iRTGs tends to increase energy benefits compared to relying solely on passive systems, ranging from 10 to 21% in savings (Muñoz-Liesa et al., 2021a; Ledesma et al., 2021; Syed and Hachem, 2019; Delor, 2011). Thus, the more sophisticated and integrated greenhouse passive and active climate controls such as building HVAC systems are, the greater the potential to recover waste energy (Ackerman et al., 2011; Aubry et al., 2017).

Important trade-offs have been also observed depending on the roof insulation values, since the increased heating benefits obtained during the cold season could also generate overheating during warmer periods. Thus, heating energy reductions from iRTGs might also lead to increased cooling requirements in the host buildings, as demonstrated by Ledesma et al. (2021). In the worst case scenario, such an increase might not compensate for heating benefits, as demonstrated in South Africa, where the annual building energy consumption increased by 3.1 and 3.5% in a poor and highly insulated roof, respectively (Hugo et al., 2021). Similarly, two hypothetical studies in school buildings in the UK and Ecuador show increased building energy needs of 3–8% (Jans-Singh et al., 2021) and 7.4% (Ledesma et al., 2021), respectively. The causes of these increased energy costs were the local climate conditions (noting that the heating needs were minimal in Ecuador and South Africa) and the iRTG in the UK, which was actively heated. However, the iRTG examples from the UK and Ecuador increased air quality and reduced peak heating loads and greenhouse energy needs to produce edible crops. Beyond RTGs, other studies recovering solar heat also showed fewer benefits in hotter climate conditions than in colder climates in Spain, ranging from 25% to 58% of energy savings when actively preheating air ventilation in buildings (Gainza-Barrencua et al., 2021). This is especially true under future climate change scenarios with expected increased temperatures, which resulted in a rise from 3.5% to 11% in the energy costs of a building integrated with a rooftop greenhouse (RTG) (Hugo et al., 2021).

Improved natural ventilation designs should be pursued to overcome overheating problems in hotter climates (Muñoz-Liesa et al., 2021a). In practice, this means improving lateral ventilation as in the case of the iRTG hosted by the Institute of Environmental Science and Technology located in Universitat Autònoma de Barcelona (ICTA-UAB, Barcelona area), which demonstrated significant energy co-benefits thanks to passive and active airflow exchanges that are continuously monitored with smart control systems (Muñoz-Liesa et al., 2021a; Muñoz-Liesa et al., 2020a; Nadal et al., 2017a; Muñoz-Liesa et al., 2020b). Thus, although passive and active operational energy could be reduced, it came at the cost of a reinforced greenhouse structure to prevent wind suction forces at the building rooftop level and a more sophisticated building climate control system (Muñoz-Liesa et al., 2021b).

Although most assessments focused on building energy benefits from integrating façade and iRTGs, bidirectional benefits to other forms of CEA (such as greenhouses and vertical farms) have also been studied. A few studies demonstrated energy savings of 4–40% when compared to soil-based greenhouses (Choi et al., 2024; Nadal et al., 2017a; Yeo et al., 2022), which reduces the overall BIA energy needs by 11.4–11.8% (Choi et al., 2024; Yeo et al., 2022). Other forms of CEA systems, such as vertical farms, have also been assessed because they can reuse waste heat from artificial lighting (i.e., LEDs). Using different energy recovery systems (e.g., heat exchangers, district heating), 12–34% of energy savings were achieved (Martin et al., 2022; Blom et al., 2023; Blom et al., 2024). This provides a deeper understanding of the active energy savings achievable through various types of building integrations (e.g., in swimming pools, office spaces, etc.) and showcases the potential of BIAs to reduce energy use in cities.

3. Methods

3.1. The ICTA-ICP building

The ICTA-ICP building hosts the headquarters of ICTA-UAB. Besides being a building with LEED Gold certification, it serves as a research platform for urban agriculture thanks to four iRTGs. Since its construction in 2014, multiple experiments have been conducted to analyze synergies between the iRTG labs and the building from multiple perspectives (Rufí-Salís et al., 2020; Parada et al., 2021; Ercilla-Montserrat et al., 2017; Llorach-Massana, 2017), all aiming to improve the resource use and environmental efficiency of agriculture and cities and to scale up these benefits elsewhere (Toboso-Chavero et al., 2018; Zambrano-Prado et al., 2021; Nadal et al., 2017b).

The building's rooftop (fourth floor) consists of (i) a central common area with four atriums, and (ii) four iRTGs distributed along the building façades (south-east, south-west, north-west and north-east, measuring 128 m^2 each), with only two iRTGs equipped with research facilities at the time this study was conducted (Fig. 1). Thermal screens insulate the rooftop greenhouses from the top and side windows and atriums when needed. The central common area is an unheated, multi-use space with less ventilation than the greenhouses, as it is mainly ventilated through zenithal windows and the four atriums. The building integrates an automatic logic control system that governs the passive and active climate via a ground source heat pump that delivers heat through active floors and air handling units (AHUs). This case study was later reconfigured to exchange their surplus low-grade heat or waste airflows via the building's HVAC system (Muñoz-Liesa et al., 2021a). The recorded

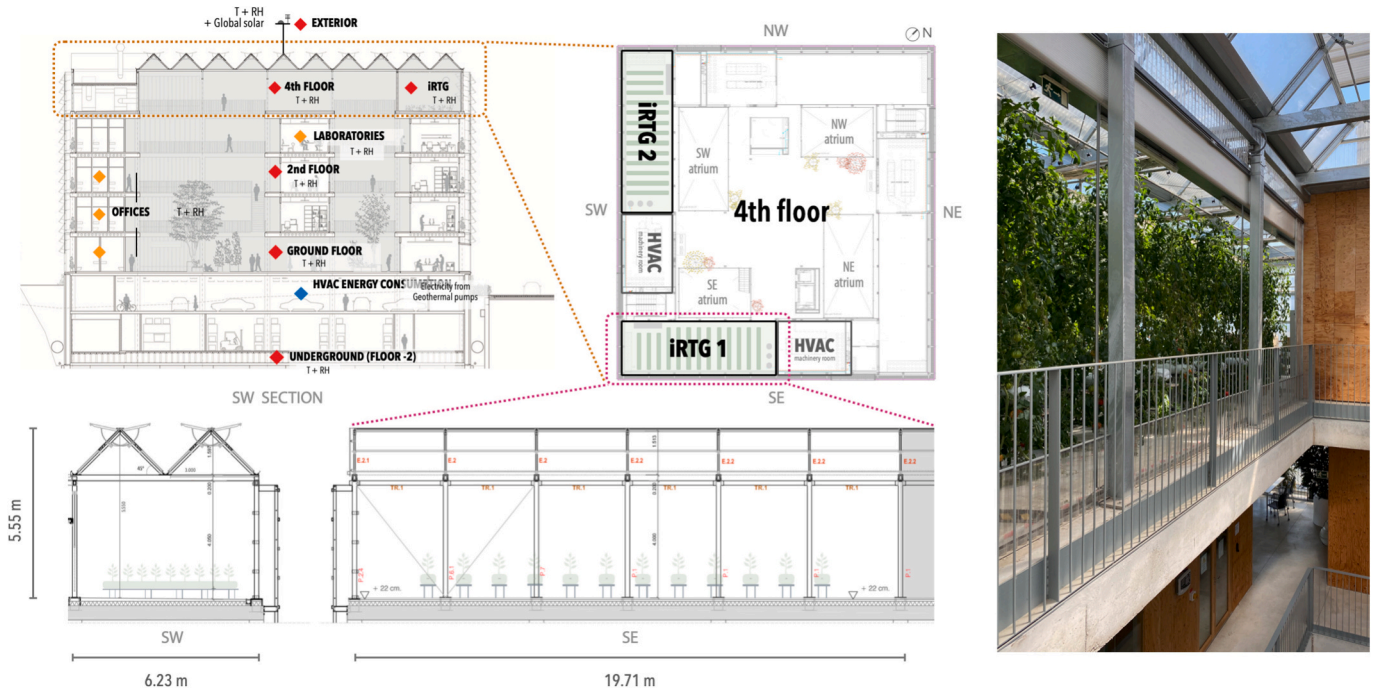


Fig. 1. Left: iRTG cross sections and floorplans, including iRTG 1 geometry and main thermal and energy recording sensors. Right: a photo from the 4th floor and the SE atrium to the iRTG 1 and the 3rd floor. Red-colored sensors indicate temperature and relative humidity sensors; energy-metered data in blue; and space identification in orange.

operational data of the building (dry-bulb temperature, relative humidity, energy meters, Fig. 1) from 2015 to 2018 was used to conduct a real-world assessment of the iRTG and quantify the energy flows exchanged, among other parameters (e.g., water, and CO_2 flows) (Muñoz-Liesa et al., 2020a).

3.2. BIA energy benefits and scenarios assessed

This study extends earlier assessments of the energy co-benefits reported for the ICTA-ICP case study (Muñoz-Liesa et al., 2021a; Muñoz-Liesa et al., 2020a; Nadal et al., 2017a; Muñoz-Liesa et al., 2020b) to integrate and comprehensively assess all energy scenarios previously assessed from a life cycle energy perspective. These previous assessments have in common the quantification of energy exchanges and modeling of the BIA system's thermal behavior by coupling real-time data from 2016 to 2018 with average yearly energy modeling results using an EnergyPlus model. Although the four iRTGs from the ICTA-ICP building face different orientations, they are physically connected along the building rooftop, share the same rooftop microclimate and are governed by the same ventilation control, so that their indoor temperature ranges are comparable; the polyethylene screens separating them do not create thermally isolated compartments. The temperature distributions recorded in the iRTGs (Muñoz-Liesa et al., 2020a) revealed synergetic effects alongside optimization challenges (including ventilation control, wintertime humidity management, and summertime thermal mass exploitation) and monthly heat exchange patterns across a full annual cycle.

Energy synergies between the building and greenhouses have been explored in the ICTA-ICP building through passive and active strategies. While passive strategies naturally occur when greenhouses are physically connected to buildings (i.e., partially integrated), offering simple direct benefits without adding operational running costs. This passive transfer combines conduction through the roof slab separating the top floor from and to the iRTG with the convective transfer of warm air through the atria and the openings connecting both spaces. Here, "passive" denotes exchanges that are not mechanically assisted, as opposed to the "active" scenarios driven by the building HVAC system. The active iRTG configuration required a tailor-made ventilation strategy to monitor and control airflow exchanges, leading to more extensive energy efficiency improvements. To evaluate all these possible energy exchange strategies in the operational phase of the BIA's life cycle energy assessment (LCEA), here we consider the energy scenarios shown in Fig. 2. We then compared the reported energy benefits from all scenarios when comparing the building and greenhouse energy demands with the equivalent building and rooftop greenhouse de-attached and isolated from each other, placing them to the ground as first assessed by Nadal et al. (2017a). Note that because each energy flow in Fig. 2 is attributed to a single beneficiary (either the building or the iRTG), no thermal energy is counted twice. The absolute energy consumption of the baseline and of the integrated configurations is reported in the Supplementary Information.

The baseline and energy scenarios considered for this assessment are:

- **Baseline scenario:** we considered the baseline situation where the building and the iRTG are isolated and placed in the ground. The ground-based iRTG would reproduce the operation of a standard venlo greenhouse actively heated to achieve the same temperatures as the iRTG actually achieves at the ICTA rooftop (with a soil conductivity of 1.28 W/mK); following the approach of Nadal et al. (2017a). Similarly, we considered the energy consumption of the ICTA building without the iRTG (Muñoz-Liesa et al., 2020a). Thus, we considered a building insulation with a standard roof structure (light-weight concrete ceiling with expanded polystyrene) achieving a U value of 0.41 W/m^2 K in line with the thermal requirements defined in the Technical Building Code. Since both are hypothetically isolated buildings, an EnergyPlus model was used to first assess the energy consumption of the iRTG (Nadal et al., 2017a) and further expanded to include the building (Muñoz-Liesa et al., 2020a), both serving as baseline assessments for scenarios 1 and 2. Importantly, the counterfactual in (Muñoz-Liesa et al., 2020a) used for scenario 2 was defined at the scale of the whole building and not only of the top floor, since the thermal influence of the iRTG propagates across the

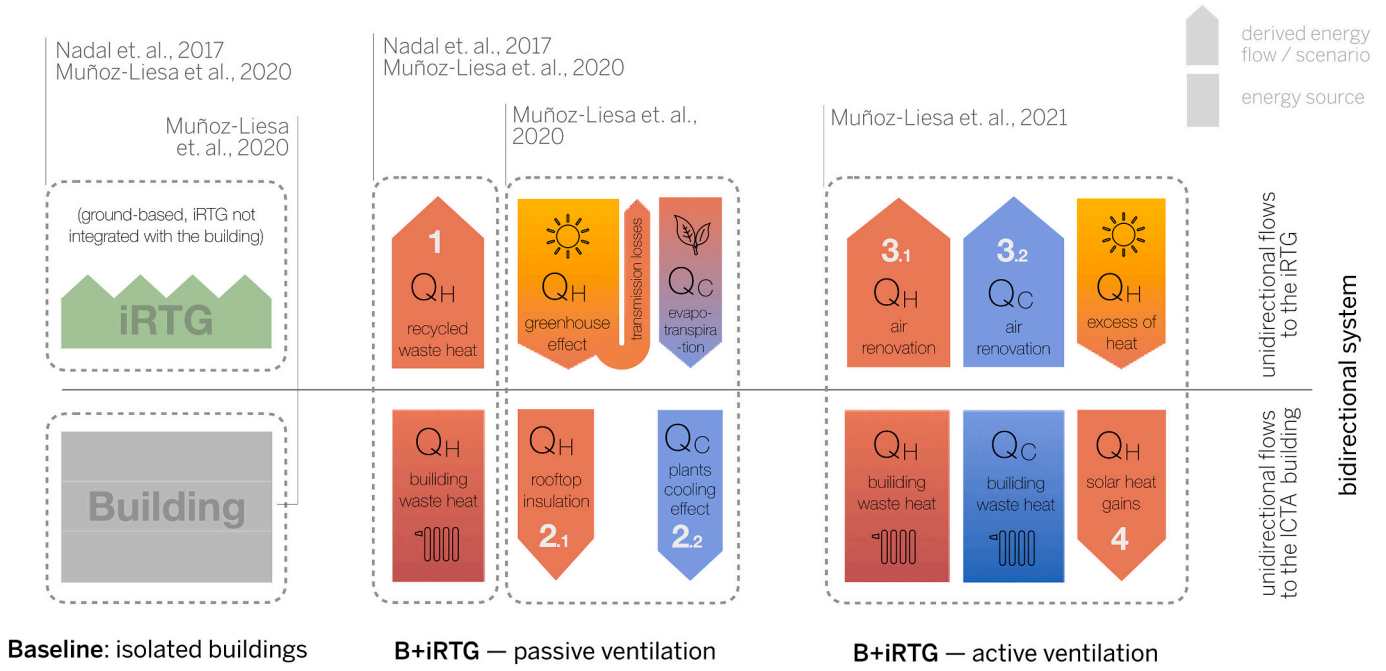


Fig. 2. Baseline and building-integrated (B + iRTG) energy scenarios considered for the LCEA, distinguishing passive (non-mechanically assisted) and active scenarios (mechanically driven exchanges via the HVAC system). Energy sources (rectangles) and the derived energy flows and scenarios (solid arrows) are represented, where arrows indicate the direction of thermal energy transfer: scenarios 1 and 3 represent flows from the building to the iRTG (building-to-greenhouse), while scenarios 2 and 4 represent flows from the iRTG to the building (greenhouse-to-building).

building levels below; all reported savings are therefore differences in whole-building (including the iRTG, when needed) energy consumption between the integrated and the baseline configurations. For scenarios 1, 3 and 4 the reported results were based on the operation of the iRTG SE-facing (Fig. 1), which incorporates bi-directional ventilation controls needed for the active scenarios. We therefore extrapolated these results to the rest of the iRTGs (measuring 512 m^2) due to the temperature range similarities found (Muñoz-Liesa et al., 2020a).

- **Scenario 1** (passive building-to-iRTG heating) examines how the envelope of the rooftop greenhouse captures the waste heat generated in the ICTA-ICP building due to the thermo-physical influence of the building on the iRTG. Building waste heat that passively rises to the top floor of the building can be thus recovered in the iRTG. This was first quantified using the first EnergyPlus model developed by Nadal et al. (2017a) resulting in 342 kWh/m^2y of equivalent thermal energy gains in the iRTG and further analyzed by Muñoz-Liesa et al. (2020a). The respective mean bias error (MBE) and the coefficient of variation of the root mean square error CV (RMSE) values reported for air temperature were 2.6% and 11.5%; whereas for humidity values were 2.9% and 15.9%, both falling within the calibration limits of ASHRAE Guideline 14.
- **Scenario 2** (passive iRTG-to-building heating) examines the insulation effect of the iRTG resulting from (i) the solar energy captured through the greenhouse effect and, scenario 2.1 (ii) the cooling effect of plant evapotranspiration, scenario 2.2. Compared to the same building configuration without the rooftop greenhouse envelope, the magnitude of passive thermal energy savings in both heat and cold flows was 120 kWh/m^2y, 112 kWh/m^2y in heating (scenario 2.1) and 8 kWh/m^2y in cooling (scenario 2.2, (Muñoz-Liesa et al., 2020a)). The EnergyPlus model by Nadal et al. (2017a) was therefore expanded to include the whole ICTA building energy-consumption data, producing MBE and CV (RMSE) values of 2.1% and 12.7% respectively; both within the ASHRAE guide 14 calibration limits.
- **Scenario 3** (active building-to-iRTG heating) evaluates the heating and cooling energy potential of using building low-grade waste heat delivered from the building's mechanical ventilation via the AHUs to the iRTGs. Thanks to their shared ventilation control, building air renovations can aid in meeting the greenhouse's thermal heating (scenario 3.1) and cooling needs (scenario 3.2). This is due to wintertime air being warmer in offices and labs than in the iRTG by a magnitude of $+5.65 \pm 2.49\,^{\circ}C$ and $+5.14 \pm 1.96\,^{\circ}C$ respectively, realizing up to 143.3 kWh/m^2y in heating (scenario 3.1) and 54.8 kWh/m^2y in cooling needs (scenario 3.2) (Muñoz-Liesa et al., 2021a). Such energy gains derive from 2016 to 2018 monitored dry-bulb temperature and relative humidity data together with the mechanical ventilation needs of the iRTG and the building, as published by Muñoz-Liesa et al. (2021a).
- **Scenario 4** (active iRTG-to-building heating), similarly to scenario 3, uses the AHUs of the building's HVAC system to mechanically extract excess warmth from the greenhouse to heat the building. This excess of solar energy remaining in the iRTG that otherwise would be vented out produced a quantifiable net benefit of 205.2 kWh/m^2y of thermal heat (without accounting the AHU's electricity needs, equivalent to 62.3 kWh/m^2 of thermal heat;Muñoz-Liesa et al., 2021a). This scenario is therefore seamlessly assessed using the monitoring data used in scenario 3, as published by (Muñoz-Liesa et al., 2021a).

In this assessment, the iRTG is therefore understood as a bioclimatic space that, when integrated into buildings, can exchange energy with the natural and the built environment to reduce energy consumption in buildings, including greenhouses. Thus, the assessment is here simplified by neglecting the tomato crop yield outputs grown in the ICTA-iRTG since 2015 (i.e., the impacts that could be attributed to tomato crop production, which would diminish energy-related impacts of BIA systems but would also lead to life cycle assessment (LCA) multifunctional issues). However, we do consider the energy-derived impacts due to tomato plant evapotranspiration that can potentially produce a cooling effect (Muñoz-Liesa et al., 2020a). Therefore, this assessment exclusively focuses on energy exchanges and saving potential when evaluating the whole life-cycle energy impacts of the building when

integrated with an iRTG. The objective of this framing is to address this assessment to building designers and managers rather than to growers, which is why the iRTG is benchmarked against other building energy-saving measures. It is also conservative, since the whole burden of the iRTG infrastructure is attributed to its bioclimatic function alone; any allocation of part of that burden to crop production would further improve the energy indicators reported here.

3.3. Life cycle energy assessment (LCEA)

Life cycle assessment (LCA) is a standardized method to evaluate environmental impacts throughout the lifetime of products and services (ISO, 2006). It has been widely used in buildings and many other analyses to assist environmental-related strategies that aim to improve a building's environmental impacts (Cabeza et al., 2014). The systemic approach for environmental evaluation in all life cycle stages allows the optimization of the construction process and determines the operational benefits by comparing multiple implementations (Ardente et al., 2011). Besides, Life Cycle Energy Assessment (LCEA) is a predecessor of LCA (Frischknecht et al., 2007), and thus, a simplified approach to track environmental impacts (due to the carbon-energy nexus) that focuses on the quantification of primary energy resources over the lifecycle of a product or service (Atmaca and Atmaca, 2015).

3.3.1. Goal and scope

In order to evaluate the LCEA of an office building coupled with an iRTG, we used the functional unit of 1 square meter of a building rooftop for a timeframe of 1 year (equivalent to 1 m^2y of the footprint area of an RTG / host building), which is a reference flow commonly used in LCEA of buildings (Ramesh et al., 2010; Cabeza et al., 2014). This choice of functional unit is further justified by the nature of the energy exchanges assessed: waste heat potentials between a BIA system and its host building depend on the volume of air exchanged, which is itself proportional to the floor area of the BIA infrastructure. Assuming typical BIA ceiling heights of 4–5 m, expressing results per m^2 of built BIA footprint (as adopted here) is consistent with LCEA and LCA conventions for buildings and enables straightforward comparisons across the BIA literature. However, to prevent the energy intensities reported here from being misread, and because part of the benefits serve the building levels below the rooftop, results are additionally normalized per m^2 of conditioned building floor area served by the iRTG in the Supplementary Information.

3.3.2. Life cycle inventory

All processes and materials within the lifetime of the iRTG were considered from raw material extraction to the end of life with a cut-off modeling approach, in which the impacts of recycling processes were allocated to the subsequent benefited product. Previous assessments of the ICTA-iRTG system have been used for the LCEA and complemented as follows. The LCEA included all energy inputs to the iRTG during its life cycle:

1. Embodied energy: Energy content in all materials and manufacturing processes used in the building and the energy requirements for construction and renovation tasks. Here, inventory data from the iRTG structure was retrieved from (Muñoz-Liesa et al., 2021b) and updated from (Sanyé-Mengual et al., 2015) to refine construction costs and material input needs according to recorded evidence. This inventory was complemented with the HVAC technical facilities needed to mechanically convey waste heat flows between the iRTGs and the building. In particular, three main energy components were included based on (Muñoz-Liesa et al., 2021a): (i) two additional AHUs, i.e. one dedicated unit per equipped iRTG installed specifically to convey air from the greenhouses to the building and therefore fully attributed to the iRTG; (ii) spiral-seam steel ductwork (500 mm diameter, 120 m total length) connecting the AHUs to the building HVAC; and (iii) auxiliary exterior valves and air intake facilities. By contrast, the pre-existing central HVAC equipment of the ICTA-ICP building, namely the ground-source heat pump and the distribution network serving offices and laboratories, falls outside the system boundary since it was already used by the building to convey the waste heat flows to the exterior. Only the incremental equipment required to realize the building-greenhouse energy exchange is allocated to the iRTG, consistently with the counterfactual defined in Section 3.2. Lifetimes of 15 years (AHUs and auxiliary equipment) and 25 years (ductwork) were assigned following standard estimations (Ardente et al., 2011). Full equipment specifications are reported in (Muñoz-Liesa et al., 2021a). Construction energy for these facilities was excluded, as installation relied primarily on manual labour at pilot scale. The remaining HVAC systems belong to the host building and fall outside the system boundaries. Note that the iRTGs are not actively heated; they benefit from building energy outflows via these components.
2. Operational energy: Energy required to maintain and operate the building, i.e., the electricity needed to operate the climate passive controls and active HVAC system. Energy exchanges between the environment and the building are taken from the building-iRTG's EnergyPlus model, considering dynamic loads under an entire year cycle of an iRTG with tomato crops as assessed by (Muñoz-Liesa et al., 2021a; Muñoz-Liesa et al., 2020a; Nadal et al., 2017a). These include solar gains, heat losses, and gains due to air infiltration, ventilation, shading devices, building obstacles, or internal gains.
3. Demolition energy: Energy required at the building's end of life as published by (Muñoz-Liesa et al., 2021b), including energy to demolish and transport building materials to recycling plants or landfill sites.

The additional inventory flows considered build on top of previous LCAs of the ICTA-iRTGs (Muñoz-Liesa et al., 2022) and are integrated here for the purpose of this assessment. It is worth mentioning that since iRTGs are an integral part of the ICTA-ICP building, 50 years of lifetime were considered for the RTG steel infrastructure and 10 years for the iRTG polycarbonate covering material. All input processes, material, and energyhin seven subsystems (Fig. 3). These included all transportation needs and end-of-life processes to capture the overall lifecycle stages of the iRTG structure. Energy expenditure to operate greenhouse passive climate controls (i.e. hardware devices and motors to run the passive installation) was integrated into the intelligent building operating system and was thus allocated according to the total passively climatized floor area, serving both iRTGs and the building (see (Muñoz-Liesa et al., 2022) for further details). No additional allocation procedures were considered; thus, building and iRTGs lifecycle energy benefits and costs were analyzed as a whole system. All background inventory data was retrieved from the ecoinvent 3.8 database (Ecoinvent, 2021).

The fertigation system, rainwater harvesting system, and other auxiliary equipment for crop operation were excluded from this assessment, as we excluded crop yields from the iRTG to focus solely on the bioclimatic benefits of the iRTG as previously mentioned. This exclusion responds to the building perspective adopted here, which is

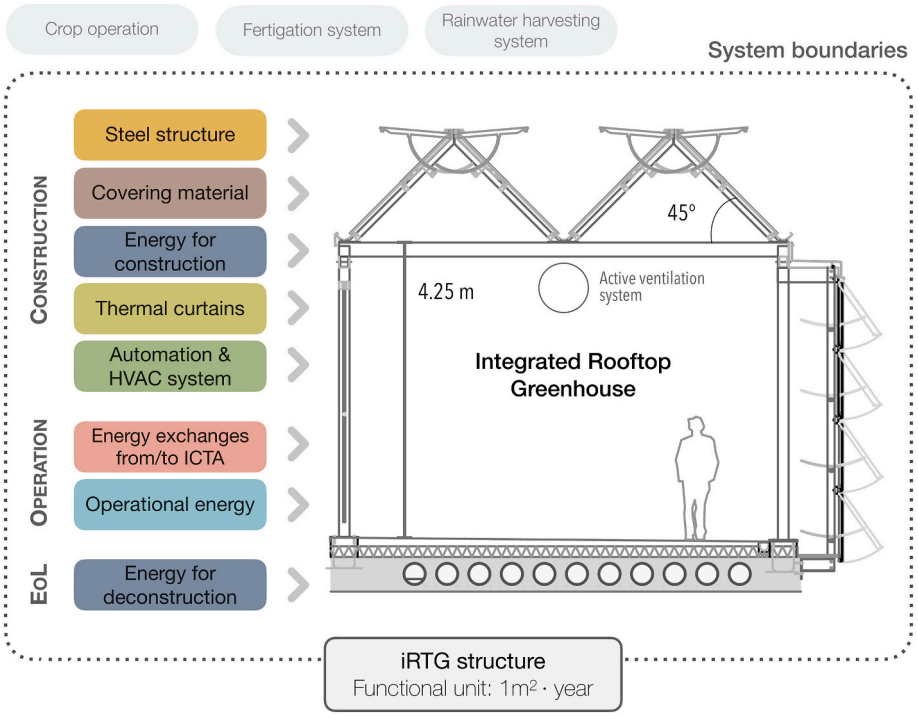


Fig. 3. System boundaries and main subsystems considered in the iRTG assessment. The seven subsystems span all life-cycle stages: (1) steel structure; (2) polycarbonate covering; (3) HVAC active components (AHUs and ductwork); (4) construction; (5) operation; (6) maintenance (covering replacement); and (7) end of life (demolition and transport). Crop-related flows (fertigation, yield outputs) are excluded from the boundary, as the assessment focuses exclusively on the bioclimatic and energy exchange functions of the iRTG.

also why the iRTG is benchmarked against other building energy-saving measures; to the fact that previous assessments of this case study have shown the greenhouse structure, which remains fixed over the 50-year study period, to dominate the cumulative energy demand, whereas cultivars and cropping calendars change repeatedly within it; and to the multifunctionality problem that including crop operations would otherwise raise. The approach is therefore conservative, since the whole burden of the infrastructure is attributed to its bioclimatic function alone and any allocation to crop production would further improve the indicators reported here. We nevertheless acknowledge that evapotranspiration, which underlies the cooling benefit of scenario 2.2, depends on irrigation and on the cultivar grown.

For comparability with building LCA practice, the seven subsystems map onto the modular structure of EN 15978 as follows: the steel structure, the polycarbonate covering and the HVAC active components correspond to the product stage (A1–A3) together with transport and installation (A4–A5); the replacement of the polycarbonate covering and of the AHUs, ductwork and auxiliary equipment at the end of their service lives corresponds to modules B2–B4; the electricity required to operate the passive controls and the active ventilation corresponds to operational energy use (B6); and demolition, transport and final disposal correspond to modules C1–C4. Modules B1, B5, B7 and D were not assessed, since no use-stage emissions, refurbishment or operational water use are attributable to the bioclimatic function of the iRTG and a cut-off approach was applied to end-of-life recovery.

3.3.3. *Impact assessment*

SimaPro 9.3 software was used together with the ecoinvent 3.8 background database. The single-issue Cumulative Energy Demand (CED, measured in MJ) was used to evaluate the primary energy use during the system's lifetime (including renewable and non-renewable energy sources) (Frischknecht et al., 2007).

3.3.4. *Energy payback time and energy return ratio*

To compare energy impacts across the building iRTG's life-cycle stages, we first converted the multiple energy flows assessed into the same physical units to calculate the equivalent energy primary demand. To this end, the coefficient of performance (CoP) of the building's HVAC heat pump was used to transform the thermal heat into equivalent electricity. These coefficients (kWh thermal heat / kWh electricity) were determined to be 3.5 and 2.5 for heating and cooling on a yearly average, respectively (Muñoz-Liesa et al., 2020a). Then, primary energy from electricity processes was computed through the CED indicator, expressed in MJ, using the European electricity mix datasets from the ecoinvent background database version 3.8, which refers to the electricity market mixes from the year 2018 (Ecoinvent, 2021).

The energy payback time (EPT) and energy return on investment (EROI) were then calculated to quantify the life-cycle energy performance of both passive (combined scenarios 1 and 2) and active (scenarios 3 and 4) ventilation configurations. These indicators were not assessed for each individual scenario due to the shared infrastructure required for both passive and active strategies in the ICTA-ICP building and the iRTGs. Such indicators also facilitate comparisons with existing energy-saving measures reported in the literature (Ardente et al., 2011).

EPT (Eq. (1)) is defined as the time needed to compensate for the primary energy used to produce a system with the system's energy savings during the operational phase, i.e., the time at which the system can offset its energy costs:

$$EPT = \frac{E_I}{E_{S,y} - E_{O,y}} \quad (1)$$

Where E_I is the energy needed to produce the iRTG infrastructure, calculated as the embodied and end-of-life primary energy invested over the whole life cycle (EN 15978 modules A1–A5, B2–B4 and C1–C4), thus excluding operational energy (module B6), which is not part of EI and is accounted for separately as EO (MJ); $E_{S,y}$ is the amount of annual primary energy savings thanks to the energy exchanged between the iRTG

and the building (in MJ/year, as the sum of the assessed scenarios, for each passive/active ventilation strategy) and $E_{O,y}$ are the iRTG annual operating primary energy costs that enable such energy symbiosis (i.e., the additional electricity needs to run the HVAC system, expressed in MJ/year). By subtracting the operational primary energy costs (E_O) from the gross primary energy savings ($E_{S,y}$), the net primary energy savings per year can be determined (Fthenakis and Kim, 2011). As mentioned, thermal energy savings of all assessed energy scenarios were translated into primary energy savings through the CED indicator, considering the energy source are ICTA-ICP's ground-source heat pumps (GSHP, CoP 2.5–3.5 for cooling and heating, respectively). Thus, this approach accounted for the electricity savings achieved via the building's GSHP due to the iRTG, while also considering that the same heat pump would heat the greenhouse if detached from the building.

Similarly, EROI (Eq. (2)) quantifies how many times the energy savings exceed the energy investment to understand the overall energy efficiency throughout the system's lifetime:

$$EROI = \frac{E_s - E_O}{E_I} \quad (2)$$

where E_S are the total primary energy savings during the iRTG infrastructure lifetime (MJ); E_O are the primary energy operational costs of the iRTG required to realize the iRTG's energy-derived benefits (MJ); and E_I is the primary energy invested needed to build the iRTG system during its lifetime (MJ). Similar to EPT, net energy savings are accounted for by subtracting operational costs from gross energy benefits.

Because both indicators are built on the same annual net energy savings and on the same energy investment, EROI and EPT are not independent: over the 50-year reference study period (RSP) adopted here, EROI = RSP/EPT. The two indicators are nevertheless reported together because EPT is the metric most frequently used in the building-retrofit literature, whereas EROI is the metric most frequently used for energy-supply technologies, and both are needed to position BIA against the benchmarks discussed in Section 4.4.

Finally, because EPT and EROI depend on a small number of influential assumptions, both indicators were recalculated over plausible ranges of the three parameters that govern the net energy balance: the CoP of the heat pump being substituted, the electricity mix used to convert electricity into primary energy (including the Spanish mix, the European one with / without Switzerland, and Switzerland mix as an example of a high-level of renewable grid), and the ventilation rate of the active configuration (0.95–3.16 air changes per hour, against the 1.59 ac/h used in the reference case). However, because the passive configuration involves no mechanical ventilation, the air change rate does not apply to this configuration, resulting into 20 different combinations against 60 combinations in the active configuration.

4. Results and discussion

4.1. Monthly energy and thermal performance

Energy scenarios of the ICTA-iRTG system are here represented on a complete annual cycle to analyze thermal benefits to both the greenhouse and the building (Fig. 4). As expected, the major greenhouse energy benefits occur as exterior and rooftop temperatures drop, when heat flows are transferred from the building to the greenhouse, especially during nighttime (representing 84% of total heat gains (Muñoz-Liesa et al., 2020a) and from November to February (scenario 1, S1). Similarly, exhaust air is mechanically transferred from offices and laboratories during nighttime (scenario 3.1), since the average mid-day rooftop temperatures reach 24 °C even during the coldest months, which minimizes daytime energy gains (Muñoz-Liesa et al., 2020a).

Passive thermal gains due to the thermal insulation of the building through the iRTGs occur from October to April (scenario 2.1), producing up to 26.2 kWh/m^2 of monthly thermal gains (Fig. 4). In contrast, the rise in building energy benefits during temperate months results from the large thermal gradient across building levels. This is due to the available solar energy gains on the rooftop combined with mild temperatures ranging from 16.6 to 19.8 °C and 18.1 to 20.9 °C in the unheated spaces from the ground and second floor, respectively. Thanks to the mechanically conveyed thermal flows from the iRTGs to the building via the integrated AHUs, net energy benefits can be realized (scenario 4). Note that these net thermal benefits (205.2 kWh/m^{2}y) already consider that 24% of equivalent thermal gains are consumed in the form of electricity to run the AHUs (i.e., consuming 62.3 kWh/m^{2}y). Moreover, the amount of recycled heat for both scenarios 3 and 4 can be increased up to 63% depending on the air changes per hour defined (here established at a standard rate of 1.59 ac/h) (Muñoz-Liesa et al., 2021a). Thus, the building air supply design will greatly influence the benefits of these waste heat exchanges. Finally, the evapotranspiration effect of plants can help to decrease the building's cooling needs when tomato crops are fully developed in the iRTG, especially from May to June, realizing up to 13.7 kWh/m^2 per month (scenario 2.2, Fig. 4).

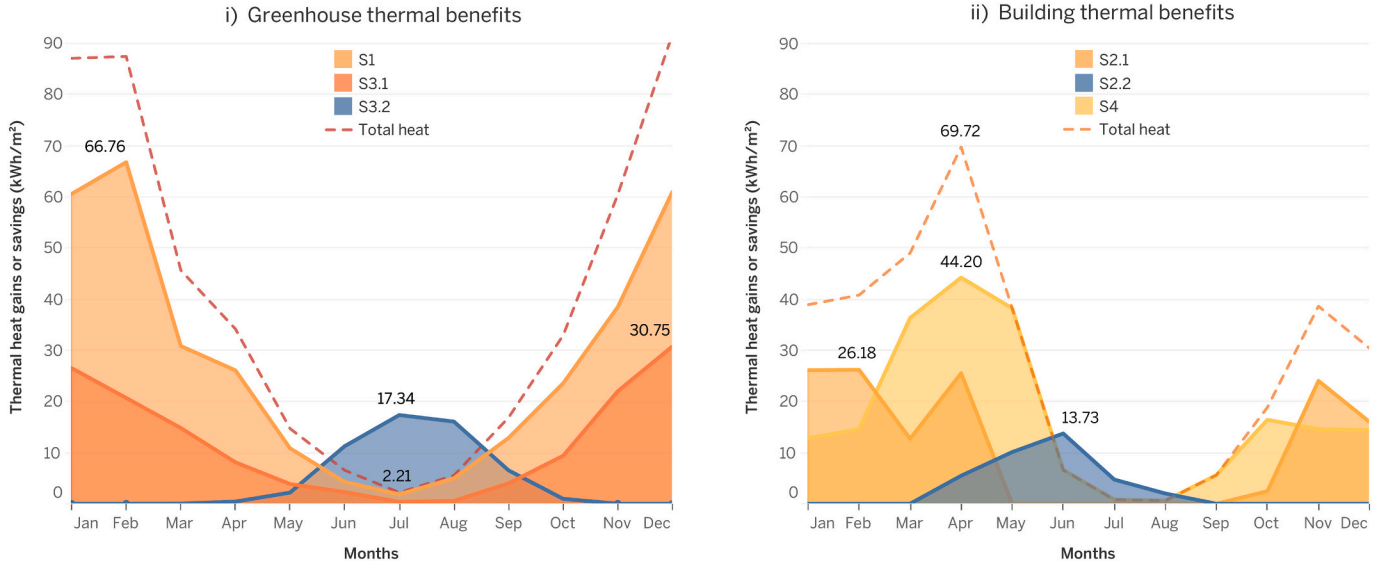


Fig. 4. Monthly ICTA-iRTGs thermal energy savings to the (i) greenhouse and the (ii) building, expressed in thermal kWh /m^2 month.

Mechanical ventilation also contributes to the cooling side of the balance. During the warm season, building air that is cooler than the greenhouse is delivered to the iRTG through the AHUs and covers part of its cooling needs (54.8 kWh/m^{2}y, scenario 3.2), thereby limiting the periods in which the greenhouse would otherwise have to be vented to the exterior. Conversely, the warm exhaust air recovered in scenario 3.1 (143.3 kWh/m^{2}y) is concentrated in the coldest months, when the greenhouse heating demand peaks.

Besides the scenarios here assessed, the existing assessments of this case study (Muñoz-Liesa et al., 2021a; Muñoz-Liesa et al., 2020a; Nadal et al., 2017a; Muñoz-Liesa et al., 2020b) also included other energy benefits of the building-iRTG system that are not considered in our evaluation since they are not quantified yet. For instance, night temperatures registered during summer nights in the iRTG were as low as 18 °C, which could cool down building-heated spaces by keeping the iRTG's automatic windows open. This would drop building temperatures and provide nighttime cooling effects to the building. Similarly, the potential of using building thermal inertia and ground-coupled natural integration of two stories below ground (−1 and −2) was also examined, since they have temperatures as low as 12 °C, which opens summertime cooling potentials for the iRTG.

4.2. Annual energy circularity performance

The ICTA-iRTG operating energy system is driven by primary electricity and solar energy sources that result in the energy exchanges and co-benefits assessed (Fig. 5, presented as the sum of all scenarios, all expressed in terms of thermal energy benefits, in kWh/m^{2}y). Both systems inevitably lose energy through envelope losses and ventilation, but these losses can be partially recovered through circular exchange strategies (Fig. 5). Thermal energy flows are exchanged simultaneously within the natural and built environment via passive and active strategies.

The main energy exchange naturally occurs with the environment when solar heat is trapped in the greenhouse as sensible heat. An average of 1630 kWh/m^{2}y of solar energy is received in the greenhouse structure, of which 890 kWh/m^{2}y (55%) are transmitted through the iRTG infrastructure (Fig. 5). Hence, the remaining 45% of the received solar energy is mainly lost due to greenhouse reflected radiation, in which covering materials are responsible for 277 kWh/m^{2}y of losses (17%). The rest of solar losses are associated with the shadows from the greenhouse structure and the building walls surrounding the iRTG (28%, 463 kWh/m^{2}y; Fig. 6). Both issues penalize crop growth (Montero et al., 2017) and the solar collector function of iRTGs (Muñoz-Liesa et al., 2021a). Of these, 890 kWh/m^{2}y are transmitted to the greenhouse, where half of the energy (445 kWh/m^{2}y) captured by plants serves as photosynthetic active radiation to promote plant growth (Thimijan and Heins, 1983). The transmitted 890 kWh/m^{2}y also contribute to heating the greenhouse, although 367 kWh/m^{2}y of thermal energy are evacuated through natural ventilation to prevent overheating. This leads to a

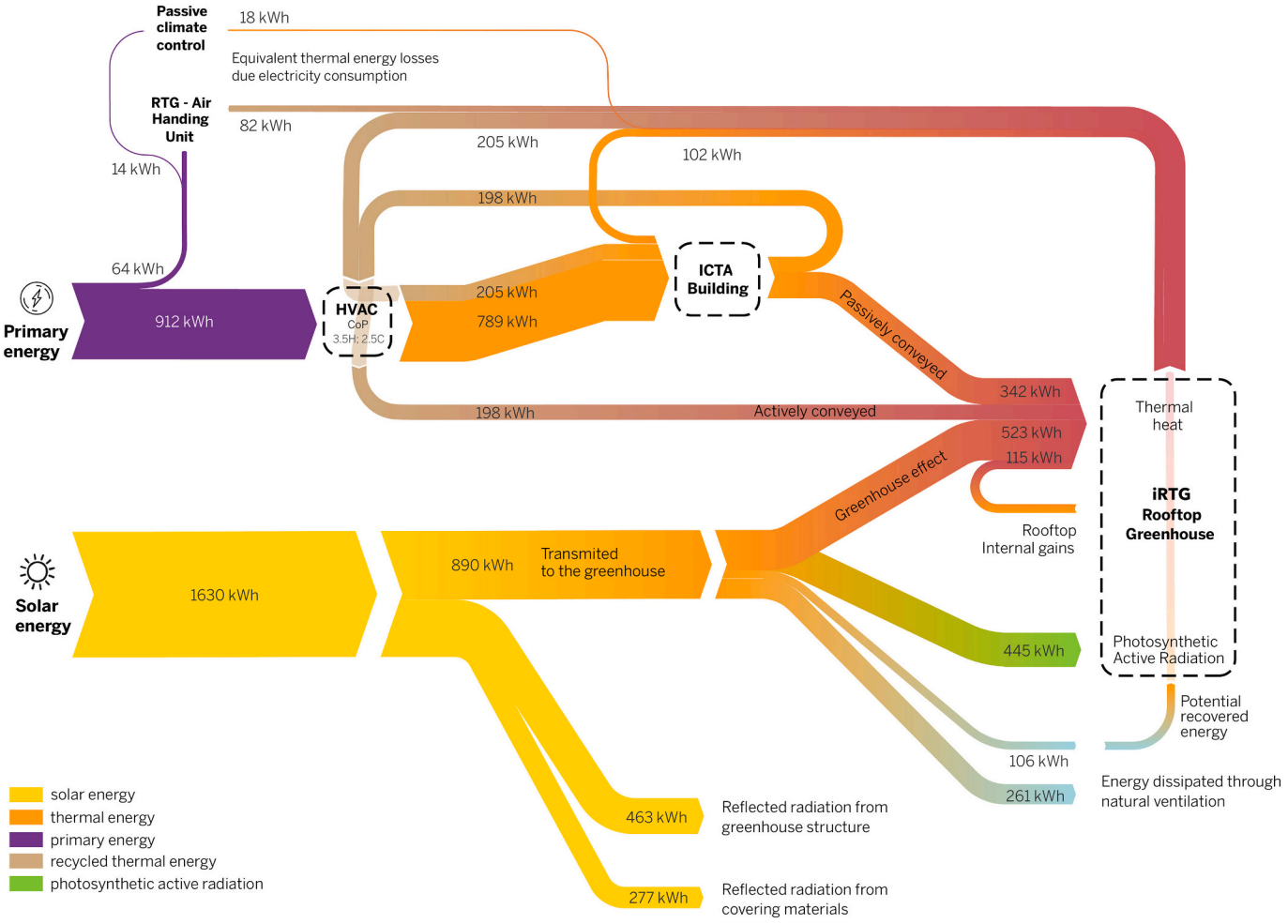


Fig. 5. Average annual building-iRTGs energy circularity and performance, including operational energy flows naturally exchanged with the environment. Photosynthetic active radiation (in green) reflects the amount of solar energy effectively used for photosynthetic activity, although it also contributes to the greenhouse effect. Units are expressed in equivalent annual thermal gains per square meter of rooftop (kWh/m^2·year).

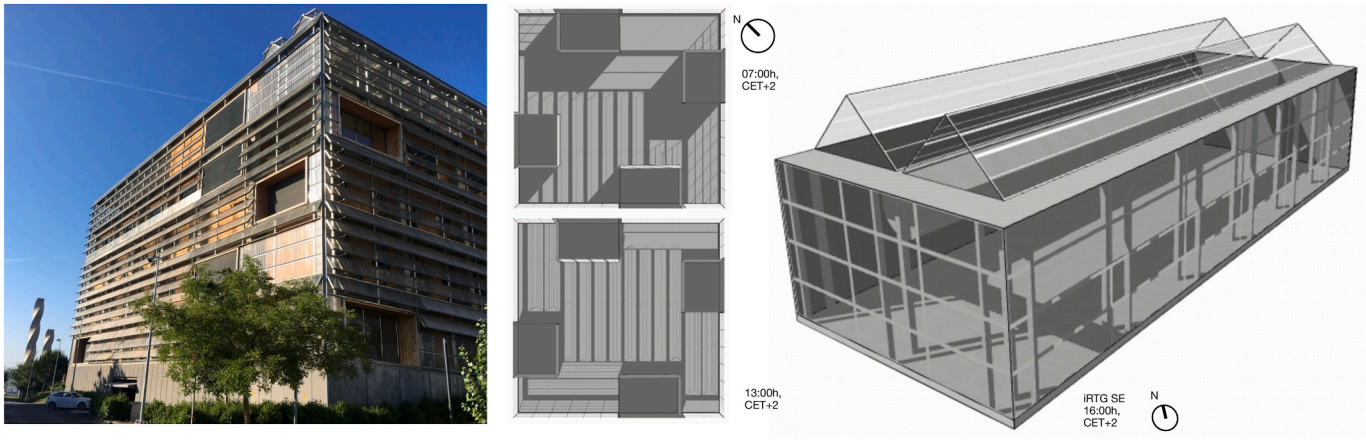


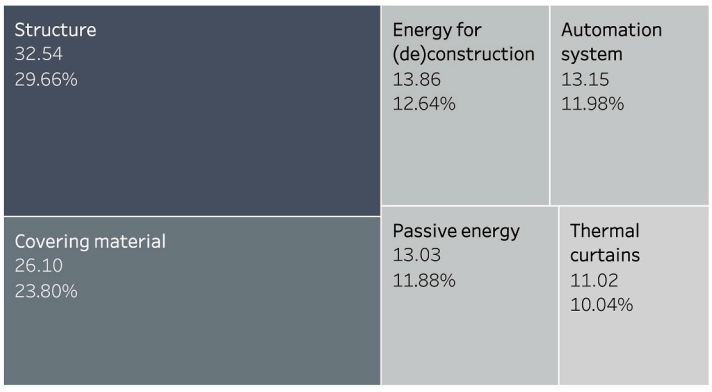
Fig. 6. iRTG shadows at different times during the day due to greenhouse structure and surrounding building walls (as modelled in Muñoz-Liesa et al., 2022, for the 23rd of June).

profitable net thermal benefit of 523 kWh/m^{2}y, which represents 32% of the total solar incoming radiation (Fig. 5). Our findings thus stress the inefficiency of the solar energy vector, which should be further improved to tap into the full potential of greenhouse energy benefits through measures like the ones mentioned below.

Managing the surplus heat is a key issue to the performance of an iRTG in a Mediterranean climate. In the ICTA-ICP case, overheating is controlled mainly through natural cross-ventilation, using automatic lateral and zenithal window openings together with thermal screens. This design choice comes at a price: the large lateral openings weaken the envelope and require the supporting structure to be reinforced (Muñoz-Liesa et al., 2021b), which increases the embodied energy of the greenhouse as calculated in this assessment. The iRTG therefore still produces overheating to the building during the warmest months, although over the year this is more than compensated by the heating benefits reported above. Other case studies with limited lateral ventilation combined with a poorly insulated roof showed this overheating problem becomes evident and can offset the heating gains (Hugo et al., 2021). A compromise consequently exists between maximizing winter heat capture and avoiding summer overheating, and it is resolved through the ventilation strategy and the structural design rather than through the covering material alone.

A possible way to overcome these inefficiencies is to improve covering material transmissivities and to design a better greenhouse integration that minimizes building internal shadows (Zambrano-Prado et al., 2021). Another solution is using active ventilation to convey the excess thermal heat that remains in the iRTG, which can be profitable in meeting the building's heating needs. Using the building's HVAC system, profitable iRTG waste airflows at ~26 °C would lead to 205 kWh/m^{2}y thermal gains (scenario 4). This would reduce greenhouse energy losses via natural ventilation to 261 kWh/m^{2}y (i.e., 28.9% reduction) and increase overall net energy benefits by 38.6% (Fig. 5). Using the same active ventilation strategy, energy gains from building air renovation need to deliver 198 kWh/m^{2}y of thermal gains to the greenhouse (scenario 3). The scenario 4 benefits come at the cost of a more controlled and closed environment that leads to the equivalent to 62.3 kWh/m^{2}y of thermal losses. Thus, the efficiency of this circular strategy is set at 76%. In contrast, scenario 3 benefits from the existing building operation control that mechanically conveys exhaust air to the exterior when air renovation is needed. Thus, recirculating air from the offices to the iRTGs is burden-free since no additional electricity inputs are required.

Automatic window openings serve two purposes: capturing building waste heat in the greenhouse and preventing overheating through natural ventilation. The energy trapped through this thermo-physical influence produces 342 kWh/m^{2}y (scenario 1, accounting for heat transfers to the iRTG as seen in Fig. 2). In contrast, the insulation effect from the greenhouse to the building saves 120 kWh/m^{2}y (scenario 2). However, this consumes 18 kWh/m^{2}y of equivalent thermal heat losses to operate the building's control system. For simplification and visualization purposes, we subtracted these equivalent energy costs from the insulation heat transferred from the greenhouse to the building (scenario 2), resulting in 102 kWh/m^{2}y of thermal heat gains. Thus, we allocated the passive climate energy expenditure to the building energy gains, although it can also be allocated to both iRTGs and building. Like the energy inputs needed for scenario 4, equivalent thermal losses are highly dependent on the CoP of the heating system being replaced, and



CED (MJ/m²·year)	Cons	Oper	Dem	Total	% Total
Material	33.8	30.3	0.0	64.1	58%
Material processing	7.0	10.4	0.0	17.4	16%
(De)construction process	2.8	9.2	1.9	13.9	13%
Operating energy	0.0	13.0	0.0	13.0	12%
End of life	0.0	0.2	0.2	0.3	0%
Transportation	0.4	0.6	0.0	1.0	1%
Grand Total	44.0	63.7	2.1	109.7	100%

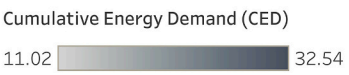


Fig. 7. Cumulative energy demand expressed in MJ/m^{2}y of iRTG for passive ventilation configuration (scenarios 1 and 2). Abbreviations: Cons: Construction phase (EN 15978 modules A1–A5), Oper: Operational phase (modules B2–B4 and B6), Dem: Demolition phase (modules C1–C4).

that will be used otherwise to produce this thermal heat. Since the HVAC system was built in 2015, its performance thus exemplifies the equivalent thermal gain or loss from relatively new HVAC systems, displaying CoP values greater than 2.5.

The primary heat source for the building is the GSHP integrated into the HVAC system. Since the thermal needs are normalized per m^2 of rooftop, the resulting values are high, as they integrate the heating needs of four stories. Lower buildings would also present major benefits, especially regarding the passive effects of iRTGs on host buildings at lower levels. Other electricity duties produce iRTG internal gains, mainly delivered from lighting, electrical equipment, and occupancy, adding up to 115 kWh/m^2y. Finally, building and iRTG account for 403 kWh/m^2y of thermal gains with active ventilation compared to 444 kWh/m^2y obtained with passive scenarios. Using active strategies, building energy needs could be reduced from 4% (passive scenarios only) to 12%, equivalent to nearly 50 MWh of annual electricity savings. As mentioned, the active ventilation energy benefits considered for the LCEA closely depend on the ventilation philosophy, which can generate varying energy savings from 8 to 19% when 0.95 or 3.16 air changes / hour are used, respectively. Thus, improved heat flow exchanges (also leading to improved air quality rates) could be considered beyond the safety value of 1.59 ac/h considered here.

4.3. iRTG life cycle energy costs – active and passive configurations

In this section, we analyze the life cycle energy costs to evaluate the energy-related environmental impacts (expressed in MJ/m^2y of primary energy demand), throughout the iRTG's lifetime with passive and active climate configurations, i.e., without accounting for the iRTG's operational benefits. The iRTG with passive climate configuration has an annual impact of 109 MJ/m^2y, in which the main contributors are the steel structure and covering material subsystems, resulting in 53.5% of total costs (Fig. 7). While the steel structure has a lifespan of 50 years, all costs occur during the iRTG's construction phase. In contrast, the polycarbonate covering material has a lifespan of 10 years, so associated costs are mainly allocated during the iRTG's operation phase due to the maintenance needs for replacing polycarbonate. Raw material production is also the main contributor to the CED (58%), followed by material processing (16%). The total amount of embodied energy is 94.6 MJ/m^2y (86.2%; although 30.3 MJ/m^2y occurs during the operational phase), while operational energy costs are 13 MJ/m^2y (11.9%). Finally, the iRTG's end of life and deconstruction phase account for only 2.1 MJ/m^2y (1.9%), which is also common in LCEA of buildings (Chau et al., 2015; Ardente et al., 2011), where the deconstruction phase typically accounts for 0.1–1% of the total life cycle energy costs (Chastas et al., 2016).

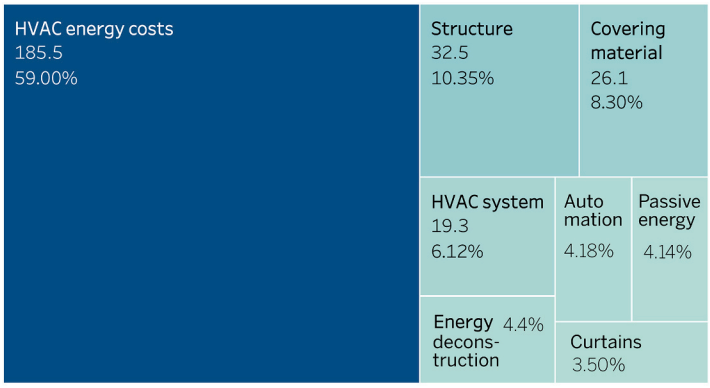
Integrating the iRTG with active ventilation strategies (scenarios 3 and 4) enhances energy circularity, which comes at the cost of raising the iRTG's CED up to 314.5 MJ/m^2y (Fig. 8). Here, additional material costs associated with the AHUs that complement the HVAC system contribute 19.25 MJ/m^2y (6.12%), which is also in line with the relative contribution of heating systems in buildings (Cabeza et al., 2014; Ardente et al., 2011). The major costs associated with operating AHUs account for 59% of CED. Together with operational energy costs, they account for 63% of total CED. Thus, embodied energy in this iRTG configuration accounts for 36.2% while energy for demolition only 0.7%.

These findings share similarities with residential and office buildings, although iRTGs are less sophisticated and provide different functions. These differences are evident when comparing energy intensities of embodied energy of buildings, which range from 1 to 12 GJ/m^2y (Chastas et al., 2016). This is up to 2 orders of magnitude compared to the iRTG passive configuration (0.11 GJ/m^2y). Passive iRTG configuration can be compared to nearly-zero-emission buildings that do not require important operational energy for heating and cooling, and thus, embodied impacts account for 74 to 100% (Chastas et al., 2016), while the iRTG represents 86.2%. In contrast, embodied energy shares of 36.2% (iRTG with active ventilation configuration) are typical of low-energy buildings (26–57%) (Chau et al., 2015). Besides, operational primary energy consumption is 198.6 MJ/m^2y and equivalent to 55.2 kWh/m^2y of electricity consumption which is as low as passive house criteria (<60 kWh/m^2y) and low-energy house threshold criteria (<75 kWh/m^2y).

4.4. Assessing BIA as an energy-saving measure

4.4.1. Energy return of the investment and energy payback time indicators

Overall iRTG CED impacts and operational benefits during the infrastructure's life cycle are presented for both iRTG passive and active ventilation iRTG configuration (Fig. 9, expressed in MJ/m^2 of rooftop and year, with additional costs colored in red text). For both configurations, energy costs are substantially lower than the benefits of energy circularity (scenarios 1–4). Material and energy costs are almost equally shared throughout the iRTG's lifetime, except for the active configuration. The passive configuration yields a total net benefit of 1371 MJ/m^2y of primary energy, translating into an EROI of 14.18, meaning that the operational benefits are 14 times larger than the energy investment in the iRTG. In turn, the EPT is 3.52 years. The active ventilation configuration of iRTGs comes at increased costs of 116 MJ/m^2y due to increased material inputs, leading to 2638 MJ/m^2y of net energy savings after subtracting the operational energy costs (199 MJ/m^2y). These raise the EROI to 22.76 and the EPT to 2.20 years, which is better than the obtained values of the passive configuration. Thus, an iRTG with integrated active ventilation strategies would be preferable as it better compensates (23 vs. 14 times) the additional infrastructure costs and



CED (MJ/m²·year)	Cons	Oper	Dem	Total	% Total
Material	42.3	41.0	0.0	83.3	27%
Material processing	7.0	10.4	0.0	17.4	6%
(De)construction process	2.8	9.2	1.9	13.9	4%
Operating energy	0.0	198.6	0.0	198.6	63%
End of life	0.0	0.2	0.2	0.3	0%
Transportation	0.4	0.6	0.0	1.0	0%
Grand Total	52.5	260.0	2.1	314.5	100%



Fig. 8. Cumulative energy demand expressed in MJ/m^2y of iRTG for active ventilation configuration (scenarios 3 and 4). Abbreviations: Cons: Construction phase (EN 15978 modules A1–A5), Oper: Operational phase (modules B2–B4 and B6), Dem: Demolition phase (modules C1–C4).

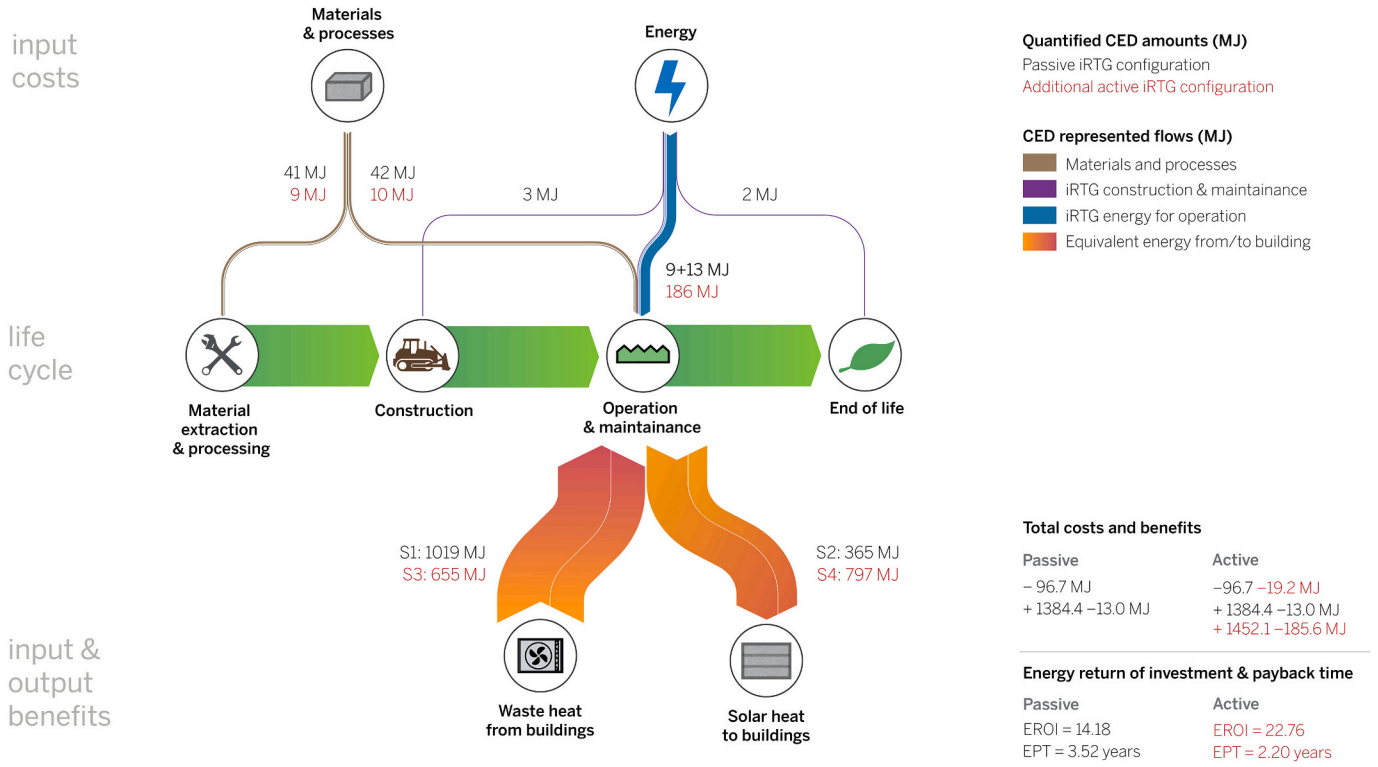


Fig. 9. Sankey diagram of the LCEA of iRTG for passive and active (both red-colored) ventilation configuration, including CED impacts and equivalent primary energy demand operational benefits per square meter of rooftop and year (MJ/m^{2}y). Green arrows represent the infrastructure lifecycle, and thus, do not quantify any energy flow.

reduces payback times by 1.32 years.

The fundamental reason why active configurations outperform passive ones lies in the thermodynamic limits of passive exchange. In passive mode, heat transfer depends entirely on the temperature gradient between the iRTG and the building, which is time-limited to nighttime and winter months (scenarios 1 and 2). This restricts the total annual recoverable thermal energy to 120 kWh/m^{2}y (scenario 2) or 342 kWh/m^{2}y (scenario 1). Active ventilation, by contrast, mechanically directs exhaust air with controlled temperature differentials of +5.14 to +5.65 °C throughout the year, enabling 198–205 kWh/m^{2}y of additional net thermal exchange beyond passive limits. Crucially, in scenario 3, the recirculated air originates from mandatory building air renovations, meaning no additional electricity input is required beyond the baseline building operation —the energy "comes for free" from a systems perspective. This is the primary driver of active systems' superior lifetime energy performance despite their higher embodied and operational costs.

4.4.2. *Sensitivity analysis: EROI and EPT values*

Besides the default parameters assessed here as a reference (concerning the HVAC's CoP, electricity mix, and the air changes per hour for the active scenarios), we performed a sensitivity analysis of each individual parameter and a full factorial analysis among the 60 and 20 combinations derived for the active and passive configurations, respectively (Fig. 10). The full factorial analysis in the active configuration resulted into a median EPT of 2.33 years (interquartile range 1.83

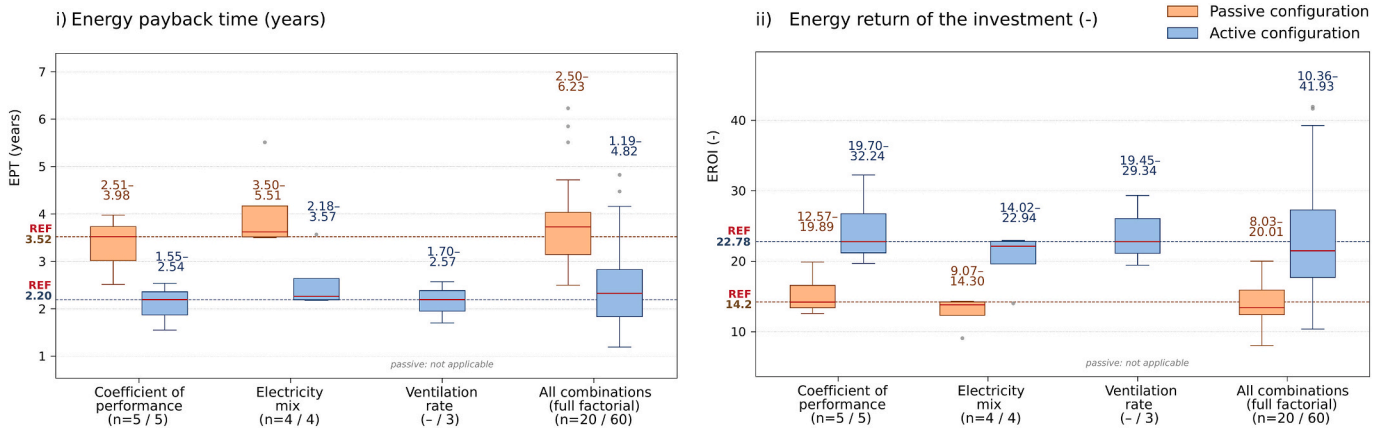


Fig. 10. Sensitivity of the life-cycle energy indicators of the ICTA-ICP integrated rooftop greenhouse using the three tested parameters affecting the (i) energy payback time and (ii) energy return on investment; for both passive configuration (orange) and active configuration (blue). Boxes span the interquartile range, the red line marks the median, whiskers extend to 1.5 times the interquartile range and grey points are values beyond that limit. Figures above each box give the minimum and maximum.

to 2.83) and a median EROI of 21.5 (interquartile range 17.7 to 27.3; full range 10.4 to 41.9). The passive configuration returned a median EPT of 3.73 years (interquartile range 3.15 to 4.03; full range 2.50 to 6.23) and a median EROI of 13.4 (interquartile range 12.4 to 15.9; full range 8.0 to 20.0), against reference values of 2.20 years and 22.8 for the active and 3.52 years and 14.2 for the passive configuration.

From the three parameters analyzed, the electricity mix is the parameter that influenced the most for both configurations, since the CED scores move from 6 to 10 MJ / kWh electricity. Thus, the least energy-intensive mix tested (Switzerland, as an example of a renewable grid) raises the payback time to 5.51 years for the passive and 3.57 years for the active configuration. The CoP spreads the EROI values, where less efficient heat pump values (i.e., CoP values from older HVAC systems) credit a larger avoided electricity demand per unit of recovered heat, improving the EROI values. The ventilation rate applies only to the active configuration and shifts its payback time between 1.70 and 2.57 years, confirming that the additional thermal exchange resulting from higher ventilation outweighs the additional fan energy required to operate it.

4.4.3. Illustrating BIA energy benefits compared to other energy-related solutions

These findings can be compared with alternative solutions to improve building retrofitting and energy self-sufficiency ratios since EPT and EROI are unphysical indicators (Weißbach et al., 2013). An iRTG is (i) a solar captor that can provide energy to the building; (ii) a passive insulation layer that provides energy savings to their host buildings; and (iii) a sink to recycle building waste heat flows. Thus, these indicators are helpful to compare the combined functions that ultimately reduce energy consumption in buildings and greenhouses. These indicators could be calculated for each scenario, but this would require dividing the infrastructure costs of the iRTG between the benefits provided to the greenhouse and the building. To avoid this complexity (i.e., dealing with multifunctionality issues in LCA), we analyze the ICTA-iRTG as a whole system without distinguishing the benefited subsystem. This approach is consistent with previous studies that have reported overall system benefits in BIA to highlight the effectiveness of energy circularity compared to current linear approaches (Choi et al., 2024; Syed and Hachem, 2019; Blom et al., 2023).

EPTs in photovoltaic panels (PV), for instance, can range from 1 to 2.7 years under the best circumstances (Fthenakis and Kim, 2011), with more frequent and realistic EPTs ranging from 2.2 to 3.2 years and up to 8 years (Sumper et al., 2011). The EPT values obtained here are therefore of the same order as those reported for PV. Other energy payback times reported range from 1.6 to 3.2 years for residential buildings constructed after the 1970s and between 3 and 5 years for older stock (Shirazi and Ashuri, 2020). Envelope insulation has been shown to pay back in about 3 years in northern Italy but only after several decades in southern Mediterranean cities, where the heating demand it offsets is small (Abd Alla et al., 2020). Deep envelope retrofits can be considerably slower still, with energy payback times of around 20 years reported for prefabricated cladding systems in Spain, the Netherlands and Sweden unless the elements are reused (Zhang et al., 2021). Thus, building insulation strategies for improving building thermal envelopes have, in general, very low EPTs, mostly ranging from 0.5 to 1.4 years but can turn as high as 26.4 years depending on the chosen material and retrofit strategies (Ardente et al., 2011). However, the same study highlighted that the combination of multiple energy-saving solutions (e.g., building insulation, PV panels, and improved insulation windows) results in payback times from 0.4 to 2.7 years. Thus, except for specific situations, the obtained EROI and EPT of the iRTG are in line with the reported best practices in the literature.

When it comes to building energy-efficiency strategies with improved HVAC systems (with heat recovery exchangers and/or more efficient equipment), payback times are even lower –between 0.04 and 0.2 years (Ardente et al., 2011). This reflects the low marginal cost of adding HVAC equipment to an existing building compared to the energy gains. Applying the same logic to the iRTG —assuming the greenhouse structure already exists and only the active system is added— yields an EPT of 0.75 years, with 76.5% of HVAC costs attributable to ductwork. Future work should therefore explore more compact active strategies (such as air-to-water heat exchangers (Doeschate, 2015)) to take advantage of the heat trapped in the greenhouse. In turn, this will facilitate building integration of such mechanisms requiring large building spaces to integrate these air heat pipes (measuring 500 mm in diameter at the ICTA-ICP building), paving the way for implementing active heat recovery strategies that are easier to integrate into the host buildings.

In accordance with Ardente et al. (2011) and similarly to the abovementioned payback times, combining building insulation strategies with improved HVAC systems, better insulated windows, or PV systems in six different case study buildings may give an EROI value range from 6 to 31. The EROI values obtained in this study, 14.18 and 22.76 for the passive and active iRTG configurations respectively, fall within that range, and the corresponding payback times of 3.52 and 2.20 years are comparable to those reported for conventional retrofit measures in recent life-cycle assessments (Shirazi and Ashuri, 2020; Zhang et al., 2021). This also aligns with the results from the sensitivity analysis: even under the least favorable combination of heat pump performance, electricity mix and ventilation rate, the active configuration paid back the energy invested in it in 4.82 years and the passive configuration returned at least 8.0 times the energy invested, so both remain within the range reported for combined building energy-saving measures across the parameters examined.

5. Conclusions

This study assessed the life-cycle energy performance of an integrated rooftop greenhouse (iRTG) at the world-first BIA demonstrator in Barcelona, combining a life-cycle energy assessment (LCEA) with a review of existing BIA studies and other building energy-saving measures to quantify how energy circularity affects life-cycle energy performance. Our findings are the following:

1. The iRTG energy savings are consistent with previous trends reported in BIA literature: a passively-integrated RTG reduces building energy demand by 4%, a value in line with the 3–15% savings reported in previous studies of rooftop and façade-integrated systems. Such benefits are constrained by the embodied energy costs of constructing BIA infrastructures, accounting for 86% of total lifecycle energy impacts. To improve passive iRTG designs, low-impact structures, and geometry and orientation that maximize solar transmittance while minimizing building self-shadings, are the key levers.
2. The iRTG actively integrated with the building's ventilation achieved 8–19% reductions in building energy demand, aligning with the 10–21% savings observed in actively ventilated systems with integrated greenhouses and up to 12–34% in other BIA forms. Despite requiring +18% of additional materials and + 187% operational inputs for the additional active ventilation equipment, the additional thermal exchange unlocked (198–205 kWh/m^2y) far exceeds the energy required to operate it, benefiting from the ventilation the building must perform anyway.
3. The active configuration reached an energy payback time (EPT) of 2.2 years (1.19–4.82 across the sensitivity analysis) and an energy return on investment (EROI) of 22.8 (10.4–41.9), against 3.5 years (2.50–6.23) and 14.2 (8.0–20.0) for the passive one. These payback times match those of photovoltaic panels (2.2–3.2 years) and the embodied energy payback of conventional retrofits, 1.6–3.2 years for post-1970s buildings and 3–5 years for older stock, and around 20 years reported for prefabricated envelope-cladding retrofits. The EROI values fall within the 6 to 31 range reported for combined

building energy-saving measures. Across the sensitivity parameters tested (heat pump performance, electricity mix and ventilation rate), the electricity mix was the most influential parameter, and active configuration outperformed the passive one in every case.

Overall, we demonstrate that diverse BIA configurations can reduce the life-cycle energy demand of greenhouses and buildings by enhancing cities energy circularity. To fully realize better integration levels and improved energy circularity efficiencies in both systems, we recommend designing BIA infrastructures to be an integral part of all building assets, such as climate controls (HVAC system, sensors, etc.) and buildings' thermal inertia. BIA thus emerges as a viable strategy to pair energy savings and food production spaces in urban areas, supporting the decarbonization of urban building stocks while creating amenity and more resource-efficient cities.

BIA designs perform unequally across contexts, and the results presented here derive from an in-depth assessment of a single case study. Future work should therefore examine how the iRTG solution behaves in other regional contexts and quantify the associated life-cycle impacts, addressing in particular transferability across climates, since the heating–cooling balance is climate-dependent and payback times for retrofit measures too; transferability across building typologies and heights, particularly for poorly insulated stocks; the multifunctional uses of BIA, by including crop yields and distributing impacts between BIA co-benefited functions; and more compact active recovery strategies, such as air-to-water heat exchangers, since ductwork alone accounts for 76.5% of the HVAC-related energy investment in this case study.

CRediT authorship contribution statement

Joan Muñoz-Liesa: Writing – review & editing, Writing – original draft, Visualization, Methodology, Funding acquisition, Formal analysis, Conceptualization. **Michael Martin:** Writing – review & editing, Funding acquisition, Formal analysis. **Anna Petit-Boix:** Writing – review & editing, Formal analysis. **Mélanie Douziech:** Writing – review & editing, Formal analysis. **Thomas Nemecek:** Writing – review & editing, Funding acquisition. **Xavier Gabarrell:** Writing – review & editing, Funding acquisition. **Eva Cuerva:** Writing – review & editing, Supervision, Funding acquisition, Data curation. **Santiago Gassó-Domingo:** Funding acquisition, Supervision, Writing – review & editing. **Alejandro Josa:** Writing – review & editing, Supervision, Funding acquisition, Formal analysis.

Declaration of Generative AI and AI-assisted technologies in the writing process

During the preparation of this work, the authors used Claude AI for language clarity in specific sections of the manuscript. The authors reviewed and edited the output as needed and take full responsibility for the content of the published article.

Declaration of competing interest

The authors declare the following financial interests/personal relationships which may be considered as potential competing interests:

Joan Muñoz-Liesa reports financial support was provided by KTH Royal Institute of Technology. The other authors declare that they have no known competing financial interests or personal relationships that could have appeared to influence the work reported in this paper.

Acknowledgments

This work received financial support from the Swedish Research Council for Sustainable Development (FORMAS) for the project "ECO-FARM CITY" (Circular vertical farms to reduce environmental impacts in cities, grant number 2022–02850) awarded to J.Muñoz-Liesa. We also thank the Ministerio de Ciencia y Innovación (MCIN/AEI/10.13039/501100011033/FEDER, UE) and the EU funding "Next Generation" for the funding of the projects MOVE4EDU (PID2021-126845OB-C21, PID2021-126845OB-C22), and BINAFET (TED2021-130047B-C21, PID2021-126845OB-C22). The authors also thank the Catalan agency AGAUR through its research group support program (2021 SGR 00734 and 2021 SGR 00341) and the finance received for the WEF4Build project (Boosting climate resilience through water-energy-food nexus based solutions). This work has also been supported by the Spanish Ministry of Economy, Industry, and Competitiveness for funding the "María de Maeztu" program for Units of Excellence in R&D (CEX 2019–0940-M). Finally, we would like to thank ICTA-UAB staff for their support. This publication reflects the authors' views.

Appendix A. Supplementary data

Supplementary data to this article can be found online at https://doi.org/10.1016/j.spc.2026.10.020.

References

Abd Alla, S., Bianco, V., Tagliafico, L.A., Scarpa, F., 2020. Life-cycle approach to the estimation of energy efficiency measures in the buildings sector. Appl. Energy 264, 114745. https://doi.org/10.1016/j.apenergy.2020.114745.

Ackerman, K., Plunz, R., Conard, M., Katz, R., Dahlgren, E., Culligan, P., 2011. The Potential for Urban Agriculture in New York City.

Ardente, F., Beccali, M., Cellura, M., Mistretta, M., 2011. Energy and environmental benefits in public buildings as a result of retrofit actions. Renew Sustain Energy Rev 15, 460–470. https://doi.org/10.1016/j.rser.2010.09.022.

Atmaca, A., Atmaca, N., 2015. Life cycle energy (LCEA) and carbon dioxide emissions (LCCO2A) assessment of two residential buildings in Gaziantep, Turkey. Energ Buildings 102, 417–431. https://doi.org/10.1016/j.enbuild.2015.06.008.

Aubry, C., Grard, B., Koegler, M., Lenouvel, V., 2017. Climate innovation potentials of urban agriculture (CIPUrA) geographic pathfinder. In: Climate-KIC & AgroParis Tech Report, pp. 1–63.

Benis, K., Gomes, R., Vicente, R., 2015. Rooftop greenhouses: LCA and energy simulation. In: Proceedings CISBAT 2015.

Blom, T., Jenkins, A., Dobbelsteen, A. van den, 2023. Synergetic integration of vertical farms and buildings: reducing the use of energy, water, and nutrients. Front. Sustain. Food Syst. 7, 1227672. https://doi.org/10.3389/fsufs.2023.1227672.

Blom, T. (Tess), Jenkins, A. (Andrew), Dobbelsteen, A.A.J.F. (Andy) van den, 2024. Synergetic urbanism: a theoretical exploration of a vertical farm as local heat source and flexible electricity user. Sustain. Cities Soc. 103, 105267. https://doi.org/10.1016/j.scs.2024.105267.

Burg, V., Golzar, F., Bowman, G., Hellweg, S., Roshandel, R., 2021. Symbiosis opportunities between food and energy system: the potential of manure-based biogas as heating source for greenhouse production. J Ind Ecol 25, 648–662. https://doi.org/10.1111/jiec.13078.

Cabeza, L.F., Rincón, L., Vilariño, V., Pérez, G., Castell, A., 2014. Life cycle assessment (LCA) and life cycle energy analysis (LCEA) of buildings and the building sector: a review. Renew. Sustain. Energy Rev. 29, 394–416. https://doi.org/10.1016/j.rser.2013.08.037.

Cerón-Palma, I., 2012. Strategies for Sustainable Urban Systems Introducing Eco-Innovation in Buildings in Mexico and Spain. Universitat Autònoma de Barcelona.

Cerón-Palma, I., Sanyé-Mengual, E., Oliver-Solà, J., Montero, J.I., Rieradevall, J., 2012. Barriers and opportunities regarding the implementation of rooftop eco.Greenhouses (RTEG) in Mediterranean cities of Europe. J. Urban Technol. 19, 87–103. https://doi.org/10.1080/10630732.2012.717685.

Chastas, P., Theodosiou, T., Bikas, D., 2016. Embodied energy in residential buildings-towards the nearly zero energy building: a literature review. Build. Environ. 105, 267–282. https://doi.org/10.1016/j.buildenv.2016.05.040.

Chau, C.K., Leung, T.M., Ng, W.Y., 2015. A review on life cycle assessment, life cycle energy assessment and life cycle carbon emissions assessment on buildings. Appl. Energy 143, 395–413. https://doi.org/10.1016/j.apenergy.2015.01.023.

Choi, E.-J., Lee, D., Lee, S.-M., 2024. Impact of building integrated rooftop greenhouse (BiRTG) on heating and cooling energy load: a study based on a container with rooftop greenhouse. Agriculture 14, 1275. https://doi.org/10.3390/agriculture14081275.

Delor, M., 2011. Current State of Building-Integrated Agriculture, its Energy Benefits and Comparison with Green Roofs—Summary.

Doeschate, T.T., 2015. The Potentials of a Rooftop Greenhouse for an Existing Mixed-Use Building towards Energy Neutrality.

Drottberger, A., Zhang, Y., Yong, J.W.H., Dubois, M.-C., 2023. Urban farming with rooftop greenhouses: a systematic literature review. Renew. Sustain. Energy Rev. 188, 113884. https://doi.org/10.1016/j.rser.2023.113884.

Ecoinvent, 2021. Ecoinvent version 3.8 Life Cycle Inventory Database. www.ecoinvent.org.

Ercilla-Montserrat, M., Izquierdo, R., Belmonte, J., Montero, J.I., Muñoz, P., De Linares, C., Rieradevall, J., 2017. Building-integrated agriculture: A first assessment of aerobiological air quality in rooftop greenhouses (i-RTGs). Sci. Total Environ. 598,

109–120. https://doi.org/10.1016/j.scitotenv.2017.04.099. https://linkinghub.elsevier.com/retrieve/pii/S0048969717309336.
European UE, 2018. Directive (EU) 2018/844 of the European Parliament and of the Council of 30 May 2018 Amending Directive 2010/31/EU on the Energy Performance of Buildings and Directive 2012/27/EU on Energy Efficiency.
European-Commission, 2016. EU Buildings Database - Energy European Commission. https://ec.europa.eu/energy/en/eu-buildings-database (accessed October 5, 2019).
Eurostat SO of the EU, 2020. Europe Built-up areas (t2020_rd110). ESMS Indicator Profile (ESMS-IP). https://ec.europa.eu/eurostat/cache/metadata/en/t2020_rd110_esmsip2.htm (accessed October 29, 2020).
Frischknecht, R., Jungbluth, N., Althaus, H.-J., Bauer, C., Doka, G., Dones, R., et al., 2007. Implementation of life cycle impact assessment methods. Ecoinvent report no. 3, Data v2.0.. Swiss Centre for Life Cycle Inventories.
Fthenakis, V.M., Kim, H.C., 2011. Photovoltaics: life-cycle analyses. Sol. Energy 85, 1609–1628. https://doi.org/10.1016/j.solener.2009.10.002.
Gainza-Barrencua, J., Odriozola-Maritorena, M., Minguillon, R.H., Gomez-Arriaran, I., 2021. Energy savings using sunspaces to preheat ventilation intake air: experimental and simulation study. J. Build. Eng. 40, 102343. https://doi.org/10.1016/j.jobe.2021.102343.
Gholami, M., Barbaresi, A., Tassinari, P., Bovo, M., Torreggiani, D., 2020. A comparison of energy and thermal performance of rooftop greenhouses and green roofs in Mediterranean climate: a hygrothermal assessment in WUFI. Energies 13, 2030. https://doi.org/10.3390/en13082030.
Gould, D., Caplow, T., 2012. Building-Integrated Agriculture: A New Approach to Food Production. Woodhead Publishing Limited. https://doi.org/10.1533/9780857096463.2.147.
Haupt, M., Hellweg, S., 2019. Measuring the environmental sustainability of a circular economy. Environ. Sustain. Indic. 1, 100005. https://doi.org/10.1016/j.indic.2019.100005.
Hugo, J., du Plessis, C., Masenge, A., 2021. Retrofitting southern African cities: a call for appropriate rooftop greenhouse designs as climate adaptation strategy. J. Clean. Prod. 312, 127663. https://doi.org/10.1016/j.jclepro.2021.127663.
IPCC, 2019. Refinement to the 2006 IPCC Guidelines for National Greenhouse Gas Inventories.
ISO IO for S, 2006. Environmental Management - Life Cycle Assessment - Principles and Framework (ISO 14040:2006).
Jans-Singh, M., Ward, R., Choudhary, R., 2021. Co-simulating a greenhouse in a building to quantify co-benefits of different coupled configurations. J. Build. Perform. Simul. 14, 247–276. https://doi.org/10.1080/19401493.2021.1908426.
Ledesma, G., Nikolic, J., Pons-Valladares, O., 2021. Co-simulation for thermodynamic coupling of crops in buildings. Case study of free-running schools in Quito, Ecuador. Build. Environ., 108407 https://doi.org/10.1016/j.buildenv.2021.108407.
Llorach-Massana, P., 2017. Mitigating the Environmental Impacts of Urban Agriculture : Innovative Materials, GHG Emissions Analysis and New by-Products.
Martin, M., Weidner, T., Gullström, C., 2022. Estimating the potential of building integration and regional synergies to improve the environmental performance of urban vertical farming. Front. Sustain. Food Syst. 6, 849304. https://doi.org/10.3389/fsufs.2022.849304.
Martínez-Blanco, J., Muñoz, P., Antón, A., Rieradevall, J., 2009. Life cycle assessment of the use of compost from municipal organic waste for fertilization of tomato crops. Resour Conservation Recycl 53, 340–351. https://doi.org/10.1016/j.resconrec.2009.02.003.
Montero, J., Baeza, E., Heuvelink, E., Rieradevall, J., Muñoz, P., Ercilla, M., et al., 2017. Productivity of a building-integrated roof top greenhouse in a Mediterranean climate. Agric. Syst. 158, 14–22. https://doi.org/10.1016/j.agsy.2017.08.002.
Montero, J.I., Antón, A., Torrellas, M., Ruijs, M., Vermeulen, P., 2012. Environmental and economic profile of present greenhouse production systems in Europe. EUPHOROS Deliverable 5, pp. 1–101.
Muñoz-Liesa, J., Chavero, S.T., Beltran, A.M., Cuerva, E., Gallo, E., Gassó-Domingo, S., et al., 2021b. Building-integrated agriculture: are we shifting environmental impacts? An environmental assessment and structural improvement of urban greenhouses. Resour. Conserv. Recycl. 169, 105526. https://doi.org/10.1016/j.resconrec.2021.105526.
Muñoz-Liesa, J., Cuerva, E., Parada, F., Volk, D., Gassó-Domingo, S., Josa, A., et al., 2022. Urban greenhouse covering materials: assessing environmental impacts and crop yields effects. Resour. Conserv. Recycl. 186, 106527. https://doi.org/10.1016/j.resconrec.2022.106527.
Muñoz-Liesa, J., Royapoor, M., Cuerva, E., Gassó-Domingo, S., Gabarrell, X., Josa, A., 2021a. Building-integrated greenhouses raise energy co-benefits through active ventilation systems. Build. Environ., 108585 https://doi.org/10.1016/j.buildenv.2021.108585.
Muñoz-Liesa, J., Royapoor, M., López-Capel, E., Cuerva, E., Gassó-Domingo, S., Josa, A., 2020b. Rooftop Greenhouses: Energy And Environmental Synergies Of Bidirectional Integration With The Building, 16, pp. 5097–5104. https://doi.org/10.26868/25222708.2019.211264.
Muñoz-Liesa, J., Royapoor, M., López-Capel, E., Cuerva, E., Ruffí-Salís, M., Gassó-Domingo, S., et al., 2020a. Quantifying energy symbiosis of building-integrated agriculture in a mediterranean rooftop greenhouse. Renew. Energy 156, 696–709. https://doi.org/10.1016/j.renene.2020.04.098.
Nadal, A., Alamús, R., Pipia, L., Ruiz, A., Corbera, J., Cuerva, E., et al., 2017b. Urban planning and agriculture. Methodology for assessing rooftop greenhouse potential of non-residential areas using airborne sensors. Sci. Total Environ. 601–602, 493–507. https://doi.org/10.1016/j.scitotenv.2017.03.214.
Nadal, A., Llorach-Massana, P., Cuerva, E., López-Capel, E., Montero, J.I., Josa, A., et al., 2017a. Building-integrated rooftop greenhouses: an energy and environmental assessment in the mediterranean context. Appl. Energy 187, 338–351. https://doi.org/10.1016/j.apenergy.2016.11.051.
Parada, F., Gabarrell, X., Rufí-Salís, M., Arcas-Pilz, V., Muñoz, P., Villalba, G., 2021. Optimizing irrigation in urban agriculture for tomato crops in rooftop greenhouses. Sci. Total Environ. 794, 148689. https://doi.org/10.1016/j.scitotenv.2021.148689. https://linkinghub.elsevier.com/retrieve/pii/S004896972103761X.
Petit-Boix, A., Leipold, S., 2018. Circular economy in cities: reviewing how environmental research aligns with local practices. J. Clean. Prod. 195, 1270–1281. https://doi.org/10.1016/j.jclepro.2018.05.281.
Proksch, G., 2017. Creating Urban Agricultural Systems. Routledge.
Ramesh, T., Prakash, R., Shukla, K.K., 2010. Life cycle energy analysis of buildings: an overview. Energy Build. 42, 1592–1600. https://doi.org/10.1016/j.enbuild.2010.05.007.
Rezaei, F., Burg, V., Pfister, S., Hellweg, S., Roshandel, R., 2024. Spatial optimization of industrial symbiosis for heat supply of agricultural greenhouses. J. Ind. Ecol. https://doi.org/10.1111/jiec.13543.
Rufí-Salís, M., Petit-Boix, A., Villalba, G., Ercilla-Montserrat, M., Sanjuan-Delmás, D., Parada, F., et al., 2020. Identifying eco-efficient year-round crop combinations for rooftop greenhouse agriculture. Int. J. Life Cycle Assess. 25, 89–576. https://doi.org/10.1007/s11367-019-01724-5.
Sanyé-Mengual, E., Oliver-Solà, J., Montero, J.I., Rieradevall, J., 2015. An environmental and economic life cycle assessment of rooftop greenhouse (RTG) implementation in Barcelona, Spain. Assessing new forms of urban agriculture from the greenhouse structure to the final product level. The. Int. J. Life Cycle Assess. 20, 350–366. https://doi.org/10.1007/s11367-014-0836-9.
Sdringola, P., Proietti, S., Desideri, U., Giombini, G., 2014. Thermo-fluid dynamic modeling and simulation of a bioclimatic solar greenhouse with self-cleaning and photovoltaic glasses. Energy Build. 68, 183–195. https://doi.org/10.1016/j.enbuild.2013.08.011.
Shirazi, A., Ashuri, B., 2020. Embodied life cycle assessment (LCA) comparison of residential building retrofit measures in Atlanta. Build. Environ. 171, 106644. https://doi.org/10.1016/j.buildenv.2020.106644.
Specht, K., Siebert, R., Hartmann, I., Freisinger, U.B., Sawicka, M., Werner, A., et al., 2013. Urban agriculture of the future: an overview of sustainability aspects of food production in and on buildings. Agric. Hum. Values 31, 33–51. https://doi.org/10.1007/s10460-013-9448-4.
Stanghellini, C., Baptista, F., Eriksson, E., Gilli, C., Giuffrida, F., Kempkes, F.L.K., et al., 2016. Sensible Use of Primary Energy in Organic Greenhouse Production.
Sturm, B., Maier, M., Royapoor, M., Joyce, S., 2014. Dependency of production planning on availability of thermal energy in commercial greenhouses - a case study in Germany. Appl. Therm. Eng. 71, 239–247. https://doi.org/10.1016/j.applthermaleng.2014.05.095.
SUEZ, 2017. The Decoset Syndicate and SUEZ Inaugurate the Heating Network in the Econotre Eco-pole: the First Tomato Greenhouses Heated by Energy Recovered from Household Waste [Press release]. https://www.suez.com/en/News/Press-Releases/Econotre (accessed January 20, 2020).
Sumper, A., Robledo-García, M., Villafáfila-Robles, R., Bergas-Jané, J., Andrés-Peiró, J., 2011. Life-cycle assessment of a photovoltaic system in Catalonia (Spain). Renew. Sustain. Energy Rev. 15, 3888–3896. https://doi.org/10.1016/j.rser.2011.07.023.
Syed, A.M., Hachem, C., 2019. Net-zero energy design and energy sharing potential of retail - greenhouse complex. J Build Eng 24, 100736. https://doi.org/10.1016/j.jobe.2019.100736.
Thimijan, R.W., Heins, R.D., 1983. Photometric, radiometric, and quantum light units of measure: a review of procedures for interconversion. HortScience 18, 818–822.
Thomas, Y., Wang, L., Denzer, A., 2017. Energy savings analysis of a greenhouse heated by waste heat. Build. Simul. https://doi.org/10.26868/25222708.2017.713.
Toboso-Chavero, S., Nadal, A., Petit-Boix, A., Pons, O., Villalba, G., Gabarrell, X., et al., 2018. Towards productive cities: environmental assessment of the food-energy-water nexus of the urban roof mosaic. J. Ind. Ecol. 23, 767–780. https://doi.org/10.1111/jiec.12829.
Torrellas, M., Antón, A., López, J.C., Baeza, E.J., Parra, J.P., Muñoz, P., et al., 2012b. LCA of a tomato crop in a multi-tunnel greenhouse in Almeria. Int. J. Life Cycle Assess. 17, 863–875. https://doi.org/10.1007/s11367-012-0409-8.
Torrellas, M., Antón, A., Ruijs, M., Victoria, N.G., Stanghellini, C., Montero, J.I., 2012a. Environmental and economic assessment of protected crops in four European scenarios. J. Clean. Prod. 28, 45–55. https://doi.org/10.1016/j.jclepro.2011.11.012.
United NU, 2007. Buildings and Climate Change. UNEP/Earthprint.
Wallgren, C., Höjer, M., 2009. Eating energy—identifying possibilities for reduced energy use in the future food supply system. Energy Policy 37, 5803–5813. https://doi.org/10.1016/j.enpol.2009.08.046.
Weißbach, D., Ruprecht, G., Huke, A., Czerski, K., Gottlieb, S., Hussein, A., 2013. Energy intensities, EROIs (energy returned on invested), and energy payback times of electricity generating power plants. Energy 52, 210–221. https://doi.org/10.1016/j.energy.2013.01.029.
Yeo, U.-H., Lee, S.-Y., Park, S.-J., Kim, J.-G., Cho, J.-H., Decano-Valentin, C., et al., 2022. Rooftop greenhouse: (2) analysis of thermal energy loads of a building-integrated rooftop greenhouse (BiRTG) for urban agriculture. Agriculture 12, 787. https://doi.org/10.3390/agriculture12060787.
Zambrano-Prado, P., Muñoz-Liesa, J., Josa, A., Rieradevall, J., Alamús, R., Gasso-Domingo, S., et al., 2021. Assessment of the food-water-energy nexus suitability of rooftops. A methodological remote sensing approach in an urban Mediterranean area. Sustain. Cities Soc. 75, 103287. https://doi.org/10.1016/j.scs.2021.103287.
Zhang, C., Hu, M., Yang, X., Amati, A., Tukker, A., 2021. Energy-carbon-investment payback analysis of prefabricated envelope-cladding system for building energy renovation: cases in Spain, the Netherlands, and Sweden. Renew. Sustain. Energy Rev. 145, 111077. https://doi.org/10.1016/j.rser.2021.111077.